Biogeochemistry (2009) 94:141–162
DOI 10.1007/s10533-009-9315-y

# The chemical character and burial of phosphorus in shallow coastal sediments in the northeastern Baltic Sea

**Kaarina Lukkari · Mirja Leivuori · Henry Vallius · Aarno Kotilainen**

Received: 28 July 2008 / Accepted: 22 March 2009 / Published online: 8 April 2009


**Abstract** The chemical composition and vertical distribution of sediment phosphorus (P) in shallow coastal sediments of the northeastern Baltic Sea (BS) were characterized by sequential extraction. Different P forms were related to chemical and physical properties of the sediments and the chemistry of pore water and near-bottom water. Sediment P composition varied among the sampling sites located in the Archipelago Sea (AS) and along the northern coast of the Gulf of Finland (GoF): the organic rich sites were high in organic P (OP), while apatite-P dominated in the area affected by sediment transportation. Although the near-bottom water was oxic, the sediments released P. Release of P was most pronounced at the site with high sediment OP and reduced conditions in the sediment-water interface, indicating that P had its origins in organic sources as well as in reducible iron (Fe) oxyhydroxides. The results suggest that even though these coastal areas are shallow enough to lack salinity stratification typical for the brackish BS, they are vulnerable to seasonal oxygen ($O_2$) depletion and P release because of their patchy bottom topography, which restricts mixing of water. Furthermore, coastal basins accumulate organic matter (OM) and OP, degradation of which further diminishes $O_2$ and creates the potential for P release from the sediment. In these conditions, an abundance of labile OP may cause marked efflux of P from sediment reserves in the long-term.

**Keywords** Baltic Sea · Coastal sea · Fractionation · Organic matter · Phosphorus · Sediment

*Present Address:*
K. Lukkari (✉) · M. Leivuori
Finnish Institute of Marine Research, Erik Palménin aukio 1, P.O. Box 140, 00251 Helsinki, Finland
e-mail: kaarina.lukkari@ymparisto.fi

H. Vallius · A. Kotilainen
Geological Survey of Finland, P.O. Box 96, 02151 Espoo, Finland

## Introduction

Like many coastal sea areas, the Gulf of Finland (GoF), which is a continuum of the Baltic Proper (BP) in the northeastern Baltic Sea (BS), and the Archipelago Sea (AS), which contains thousands of small isles southwest of Finland, are eutrophied. Coastal sea areas receive most of the nutrients discharged from the terrestrial environment via rivers and estuaries (and groundwater discharge), and algal blooms often cause the most harm in coastal areas, hindering their recreational and economical use. In the GoF and AS, the main sources of phosphorus (P) are agriculture, municipal wastes, and fish farming (Bonsdorff et al. 1997; HELCOM 2003). However, P is also released from reserves accumulated in bottom sediments (e.g. Emeis et al. 2000). P bound to

iron (Fe) oxyhydroxides in the sediment is released when Fe is reduced due to oxygen ($O_2$) depletion in the near-bottom water (Einsele 1936, 1938; Mortimer 1941, 1942). In addition, release of organic P (OP) can be enhanced under $O_2$ depletion (Ingall et al. 1993; Ingall and Jahnke 1994; Ingall and Clark 1998). Despite their shallowness, some areas in the AS and northern coast of the GoF are seasonally hypoxic ($O_2 < 2$ ml $l^{-1}$) (Bonsdorff et al. 1997; Virtasalo et al. 2005; Vallius 2006; Kotilainen et al. 2007). Variable bottom topography (Winterhalter et al. 1981) creates sub-basins sheltered from strong water currents, and they gather organic matter (OM). Microbial degradation of OM consumes $O_2$, especially in summer, and further releases Fe-bound P. Degradation of organic P compounds also releases phosphate ($PO_4$-P), making it available to bacteria and algae.

In addition to the concentration of $O_2$, sediment P release depends on the chemical character and binding forms of P and on sediment properties. In fact, P release also occurs in oxic conditions (Lee et al. 1977; Boström et al. 1982). Mineralization- or reduction-released $PO_4$-P in sediment pore water diffuses to the near-bottom water if it is not bound e.g., to Fe or aluminium (Al) oxyhydroxides, or incorporated into organisms. Although the benthic animals mix and oxidize the sediment surface, improving its P binding ability and possibly also enhancing authigenic Ca–P formation deeper in the sediment (Slomp et al. 1996a), deep burrow channels can enhance pore water $PO_4$-P release (Petr 1977; Aller 1988; Hietanen et al. 2007). In addition, anion competition (e.g., silicate, $SiO_4$-Si, and organic acids) and an increase in pH may result in release of P from metal oxides (Hingston et al. 1967; Ryden et al. 1987; Koski-Vähälä et al. 2001). Eutrophication and hypoxia are common problems in many shallow coastal environments. However, the present knowledge on the chemical character of sediment P in these areas, which could help in quantifying the processes in P cycling and seeking for applicable protection measures, is inadequate.

Fractionation is a commonly used method to characterize P in aquatic sediments. It separates P into several forms according to solubility and reactivity against various reagents. For example, Hieltjes and Lijklema (1980), Van Eck (1982), Pettersson et al. (1988), and Ruban et al. (1999) have discussed and compared different methods. Despite the role of sediments in P loading and the importance of sediment P forms for its release, P fractionation studies in coastal areas of the BS are still few. Moreover, they use different methods, making comparison of results difficult. Redox-dependent P is shown to be abundant in oxic archipelago sediments and near-shore areas in the western BP (Carman and Jonsson 1991) as well as in surface sediments in the Gulf of Riga (Aigars 2001) and Kiel Bight (Balzer 1986). In Aarhus Bay, Fe-bound P and apatite-P are the most abundant P forms (Jensen and Thamdrup 1993; Jensen et al. 1995). Frankowski et al. (2002) reported that Ca-bound P dominated, followed by Fe- and Al–P in the Pomeranian Bay, while residual P, Fe–P, and Al–P were abundant on the northeastern coast of the GoF (Lehtoranta 1998), although, in that study, Al–P may have been overestimated (Chang and Jackson 1957; Williams et al. 1971a). Virtasalo et al. (2005) found that in the surface sediments of AS, OP dominated, followed by detrital apatite-P, redox-sensitive P, and authigenic apatite-P.

We examined the chemical composition of P in different sediment types in oxic shallow coastal areas in the AS and northern GoF in order to evaluate the potential for release or burial of sediment P, and thus, the potential affect on eutrophication. We also studied the chemistry of the sediment, pore water, and near-bottom water to clarify the behaviour of P at the sediment-water interface. This study of coastal sediments overlain by oxic near-bottom water was made using the same methods as previously in studies of estuaries and poorly oxygenated open sea sediments in the northeastern BS (Lukkari et al. 2008, submitted), which allows comparison of the results.

## Materials and methods

### Research area and sediment types in the research area

The mean water depth of the GoF (area 29 571 $km^2$) is only 37 m and the deepest basin is 123 m deep (Alenius et al. 1998). Salinity is low (6–10 PSU in the bottom water) but the bottom topography at the mouth of the GoF allows intrusions of bottom water of higher salinity from the BP, creating salinity stratification. In the AS (area 8,300 $km^2$), salinity

ranges from 4 to 7 PSU and the mean water depth is 23 m (Winterhalter et al. 1981; Virtasalo et al. 2005). Water depth at the sampling sites ranged from 28 m (BISA1, Fig. 1) to 53 m (C74); thus, they are all located above the halocline that varies from about 60 to 80 m in depth (Kullenberg 1981; Alenius et al. 1998), although shallow coastal basins can be thermally stratified (Virtasalo et al. 2005; Kotilainen et al. 2007). Sites AS2, C63, BISA1, and BZ1 were our main study sites and they were investigated in more detail than the rest of the sites (C55, C74, and C6).

The basement in the study area consists of Paleoproterozoic crystalline bedrock (Koistinen et al. 2001), generally covered by till. Till and bedrock are often covered by late glacial and postglacial clays, silts, and sand (Winterhalter et al. 1981). Modern sediments in the northeastern BS are mainly muddy clays rich in humic matter and Fe but

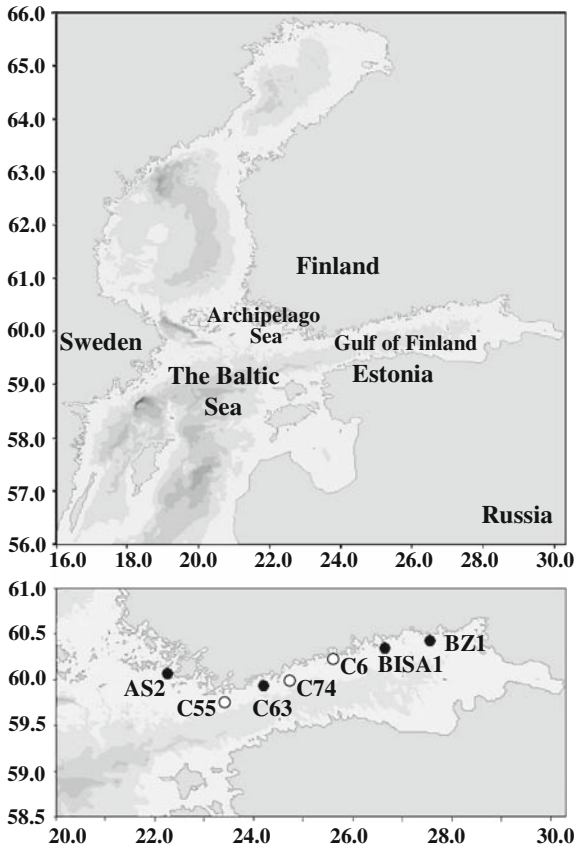


**Fig. 1** The research area and locations of the sampling sites in the Gulf of Finland and the Archipelago Sea, the Baltic Sea. Locations of the main study sites are represented by *black dots*

poor in calcium carbonate ($CaCO_3$) (Winterhalter et al. 1981; Conley et al. 1997; Carman 1998). The concentration of total carbon (TC) is practically the same as that of total organic carbon (TOC) in the study area. All of the main sampling sites (AS2, C63, BISA1, and BZ1) were considered oxic, because dissolved $O_2$ in the near-bottom water was >2 ml $l^{-1}$.

The sediment surface (ca. 1-cm layer) at site AS2 was brown, fluffy mud. The muddy clay below that had unclear black and gray laminas. At site C63, a brown 1-cm surface layer covered grayish black, homogeneous muddy clay that could be sub-sampled only down to 15 cm. The fluffy, black, clayey mud at BISA1 had white bacterial growth on top of it. The muddy clay below that had black and gray laminas. At BZ1, a clayey mud surface with a thin brown layer covered laminated (black and gray) muddy clay. At BISA1 and BZ1, the water content was 90–96% in the topmost 5 cm layer and decreased to 70–80% at 25 cm depth. At AS2 and C63, the water content was 80–89% in the surface layer and it decreased to 75 and 40%, respectively, at 15 cm depth. Muddy clay sediments at sites C55 (Vallius 2006) and C74 were partly laminated, while that at C6 was black and homogeneous. Sediment was reduced at C55 but C74 had a 2-mm brown layer on top.

## Sampling

Sampling sites were selected based on data from echo sounding surveys. Sediment samples from the main study sites were collected on three cruises of the r/v Aranda: in August 2003 (AS2), April 2004 (C63), and August 2004 (BISA1 and BZ1). Six sediment samples were taken with a Gemax gravity corer (two acrylic cylinders, inner diameter 9 cm, length ca. 60 cm) from each site. Two cores were put vertically on a slicing table and covered with a glove bag tightly joined to another glove bag. The glove bags were sealed and filled with nitrogen ($N_2$, purity 99.5%) until the $O_2$ content was <5–10% (detected with Gas Alert detectors calibrated against fresh air, $O_2$ content 20–21%). After the water column above the sediment (5 cm) had been sampled and the rest of the water removed, the core was cut into 1-cm slices (from 0–10, 14–15, 19–20, and 24–25 cm depth intervals, except down to 15 cm at C63). The samples from the two parallel cores were pooled and sealed in plastic containers in the second glove bag (cooled with ice,

$O_2 < 5\%$), and the containers were vacuum packed (Tecla s.n.c Vacum 33) into gas-tight plastic bags (filled with $N_2$) and stored at 5°C (in the dark). Another pair of sediment cores were sectioned with the same intervals (except down to 45 cm, 5-cm intervals, for cores from BZ1) without $N_2$ and immediately frozen (−18°C).

The rest of the sites were sampled from r/v Kaita in July 1998 (C6) and September 2002 (C55 and C74) with a Gemax corer. Sediment cores were sectioned (without $N_2$) into plastic bags and stored at ca. 5°C (in the dark). At C55 and C74, cores were sectioned at 1-cm intervals down to 5-cm depth, below which 1-cm sections were taken at every 5-cm of depth, down to 45 and 40 cm, respectively. The core from site C6 was sectioned at 1-cm intervals down to 25 cm depth (1-cm sections were also taken at 29–30 and 34–35 cm depths). The water depths at sites C55, C74, and C6 were 46 m, 53 m, and 38 m, respectively.

## Analytical methods

### *Water column and pore water samples*

Near-bottom water and pore water were sampled at the main sites (AS2, C63, BISA1, and BZ1). Water column salinity, temperature, and dissolved $O_2$ were determined with a CTD instrument (Sea-Bird Electronics). Dissolved P ($PO_4$-P), N as nitrate ($NO_3$-N) and ammonium ($NH_4$-N), silicate ($SiO_4$-Si) and total P (TP) and N (TN) (after acid persulfate digestion) were determined onboard with an autoanalyser (Lachat QuickChem 8000) (Hansen and Koroleff 1999). Dissolved $O_2$ in the near-bottom water (5 cm above the sediment) was determined by Winkler titration (Grasshoff 1983). The near-bottom water was also analysed for dissolved P and N (filtered with 0.4 μm Nuclepore polycarbonate (PC) membranes) and TP and TN (unfiltered) as above. Incubation-derived $PO_4$-P flux was determined incubating four intact replicate sediment cores at in situ temperature (in dark, stirring the water column). $PO_4$-P was determined at the beginning and after 5-h incubation and the $PO_4$-P flux was calculated per surface area on the basis of the concentration difference.

At AS2, BISA1, and BZ1, pore water in the surface sediment (down to ca. 4-cm depth) was collected in an argon (Ar) atmosphere (atm) using a hydraulic squeezer (Bender et al. 1987; Mäkelä and Tuominen 2003) and immediately analysed on board for dissolved nutrients. The sampling interval (in mm) is calculated from the porosity of the sediment, the volume of collected pore water, and the radius of the cylinder of the corer (Bender et al. 1987; Mäkelä and Tuominen 2003). The problems caused by oxidation (Bender et al. 1987) were diminished by starting the sampling immediately after lifting the core and using Ar-shielding. In addition, at C63, BISA1, and BZ1, pore water was separated from deep sediment profiles by centrifuging 1-cm sections of sediment (the same depth intervals as above, 4,000 rpm, 30 min). Sediment sectioning, transfer into tubes, and filtration of the supernatant (0.4 μm Nuclepore PC membranes) were carried out under $N_2$ atm in a glove bag ($O_2 < 5\%$). A portion of each pore water samples was acidified (65% s.p. nitric acid, pH < 2, storage at 5°C) and later analysed for total dissolved Fe and manganese (Mn) by ICP-AES. The detection limits for Fe and Mn were 0.8 and 0.3 μmol $l^{-1}$ and recovery was 113% for both metals.

### *Sediment*

The frozen sediment cores from the main sites were freeze-dried and homogenized (Pulverisette 5) for total analysis of P ($TP_{sed}$), Fe, Mn, Al, and Ca. The concentrations of the elements were measured with an ICP-AES (TJA-25, Thermo Jarrell Ash) after digestion (fluoric acid, aqua regia, and boric acid in a microwave oven, CEM-205) (Leivuori 2000, modified from Loring and Rantala 1992). In the reference materials (Buffalo River sediment 8704, not certified for P, and MESS-3, NRCC, informative value for P), the recoveries were 110% for P and 96–110% for Fe, Mn, Al, and Ca. Detection limits for P, Fe, Mn, Al, and Ca were 0.5, 0.4, 0.1, 0.4, and 1.3 μmol $g^{-1}$, respectively.

At the four main sites, redox potential, pH, and temperature were determined from one core by pushing electrodes (SenTix Sur for pH, SenTix ORP for redox, and TFK325 for temperature) into the sediment. The measurement was started above the sediment and continued into the sediment to 10 cm depth. The redox potential values are considered descriptive only because they do not accurately describe the processes in the sediment (Stumm and Morgan 1996; Drever 2002) and some of the anoxic

layers may contain hydrogen sulphide deleterious to common electrodes.

For sites AS2, BISA1, and BZ1, $^{137}Cs$ activity was determined at the Finnish Radiation and Nuclear Safety Authority (as described in Kyzyurov et al. 1994; Kankaanpää et al. 1997; Mattila et al. 2006) for sediment dating and calculation of sediment accumulation rate (SAR). $^{137}Cs$ peak values in the study area indicate sediment deposition in 1986 (fallout after the Chernobyl accident). The SAR value for site AS2 is from Mattila et al. (2006), while SAR estimates for the other sites were made at the Geological Survey of Finland (GTK). Particle size distribution was determined at GTK by sieving (particles >60 μm) and with a Sedigraph analyser (<60 μm). Sediment total carbon ($TC_{sed}$), nitrogen ($TN_{sed}$), and sulphur ($TS_{sed}$) were determined with a LECO CNS-2000 analyser at the Pirkanmaa Regional Environment Centre. Sediment samples from sites C55, C74, and C6 were freeze-dried and sieved (<2 mm) before analysis of $TP_{sed}$ by ICP-AES after fluoric acid and perchloric acid digestion at GTK. For these sites, $TC_{sed}$ (LECO CHN-600 analyser) was determined at GTK.

*P fractionation*

P fractionation (Table 1) was done at sites AS2, C63, BISA1, and BZ1. A quantity of fresh sediment equivalent to 0.500 g dry matter (DM) was extracted serially with 50.0 ml of various solutions following the scheme of Jensen and Thamdrup (1993), which is modified from the scheme of Psenner et al. (1984). The Jensen and Thamdrup (1993) method was slightly modified further by replacing step V with the corresponding step in SEDEX-method (Ruttenberg 1992). A detailed description of the extraction is given in Lukkari et al. (2007). Briefly, in step I, NaCl separates loosely-bound and pore water P (referred to later as NaCl-iP). In step II, NaBD (pH 7) removes redox-sensitive P bound to hydrated oxides of reducible metals, mainly Fe (NaBD-iP). In step III, NaOH extracts P bound to hydrated oxides of Al and other metals not reduced in step II (NaOH-iP) and the labile OP (NRP). In step IV, HCl dissolves Ca-bound P, mainly apatite-P (HCl-iP). Steps I–IV include rinsing steps and steps I–II were extracted in $N_2$-atm in a glove box to avoid oxidation. In step V, the sediment residues are dried (24 h, 105°C), combusted, and extracted with HCl to separate the refractory OP (Res-P). Filtered (0.4 μm Nuclepore PC membranes) extracts were analysed for $PO_4$-P and unfiltered extracts for TP (after acid persulfate digestion; Koroleff 1983). The filtered and acidified extracts from steps II and III were also analysed for total dissolved ($T_{diss}$) Fe, Mn, Al, Ca, Mg, and Si by ICP-OES at the Institute for Environmental Research (University of Jyväskylä). Detection limits were 10 mg $l^{-1}$ for Fe, Mn, Al and 20 mg $l^{-1}$ for Ca, Mg, and Si.

The P fractions can be divided into mobile P (including NaCl-iP, NaBD-iP, and NRP) and immobile P (including NaOH-iP, HCl-iP, and Res-P; Jensen et al. 1995). However, the term "reactive P" (Froelich 1988; Louchouarn et al. 1997; Delaney 1998; Anderson et al. 2001) was chosen instead of "mobile P". Burial fluxes for P were calculated by multiplying the immobile P at the surface by the SAR values. Because of diagenetic processes in the sediment and variable SAR values among the sites, the surface layers do not represent newly deposited material or that deposited during one year. However, P concentrations in the surface layers were used in

**Table 1** Outline of the P fractionation scheme

| Step | Extractant | Separated P fraction |
|---|---|---|
| I | 0.46 M sodium chloride (NaCl), 1 h | Pore water P, loosely-bound P (NaCl-iP) |
| II | 0.11 M sodium dithionite in sodium bicarbonate (NaBD), 1 h | P bound to redox-sensitive metals (Fe and Mn) (NaBD-iP) |
| III | 0.1 M sodium hydroxide (NaOH), 18 h | P from Al oxides, non-reducible Fe-compounds (NaOH-iP) and labile organic P (NRP) |
| IV | 0.5 M hydrochloric acid (HCl), 1 h | Apatite and other inorganic P (HCl-iP) |
| Ignition of the sediment residue: 2 h at 550°C | | |
| V | 1 M hydrochloric acid (HCl), 16 h | Residual, mainly refractory organic P (Res-P) |

calculations because they were the best estimates available from this data. The burial efficiency of total P in the sediment was expressed as the proportion of immobile P at the surface layer as percentage of the total extractable P ($TP_{extr}$), i.e. the sum of P in the separate fractions (Jensen et al. 1995). The burial efficiency here includes all buried P forms, thus, it is not comparable to burial efficiency of reactive P. The long-term average for the annual efflux of sediment P was calculated from the concentration difference between reactive P in the surface layer and at the nearest sample depth to the $^{137}Cs$ maximum (i.e., year 1986) at each site, and dividing that by the age difference (in years). The P effluxes calculated from solid phase data represent minimum estimates (Krom and Berner 1981).

### Statistical analyses

Statistical analyses were carried out using the mixed model (run with the SAS program) to determine which variables (elements in sediments and extracts) explain the P fractions. The mixed model was chosen because observations were correlated (different variables were determined from several depth layers at each sampling site). The sampling site was set as a random variable, and the sediment depth layer was treated as a repeated factor (autoregressive structure in the longitudinal data assumed). The dependence was tested with the *F*-test (significant when $\leq 0.050$). Parameters for the mixed model analysis were chosen on the basis of their mutual relationships, which were studied with the Pearson correlation (with Bonferroni probabilities) and by principal components analysis (PCA, with Varimax rotation, carried out on the basis of Spearman correlations) (run with the SYSTAT program).

## Results

### Water column and pore water

Table 2 describes the chemistry of the near-bottom water. Dissolved $O_2$ was highest at site C63 and lowest at BZ1. In contrast, $PO_4$-P was highest at BZ1 and lowest at C63. Site BZ1 was also highest in other dissolved elements. Incubation-derived $PO_4$-P flux was highest at BISA1. It was always positive i.e., directed from the sediment to the water. Salinity was around 6 PSU at all sites.

**Table 2** Parameters describing properties of the sampling sites and near-bottom waters

| Parameter | AS2 | C63 | BISA1 | BZ1 |
|---|---|---|---|---|
| Water depth (m) | 47 | 45 | 29 | 40 |
| *Near-bottom water* | | | | |
| $O_2$ (ml $l^{-1}$) | 4.9 | 8.6* | 3.8 | 3.4 |
| $PO_4$-P (μmol $l^{-1}$) | 1.4 | 1.0 | 2.8 | 4.3 |
| TP (μmol $l^{-1}$) | 3.2 | 1.9 | 6.5 | 5.9 |
| $SiO_4$-Si (μmol $l^{-1}$) | 16.9 | 15.8 | 26.2 | 37.8 |
| $NO_3$-N (μmol $l^{-1}$) | 3.6 | 3.3 | 5.4 | 11.9 |
| $NH_4$-N (μmol $l^{-1}$) | 3.5 | 0.6 | 8.0 | 10.8 |
| TN (μmol $l^{-1}$) | 34.4 | 27.7 | 43.2 | 41.4 |
| $PO_4$-P flux (μmol $m^{-2}$ $day^{-1}$) | 46 | – | 1,065 | 193 |
| $Fe_{diss}$ (μmol $l^{-1}$) | 8.9 | 0.5 | 1.1 | 12.3 |
| $Mn_{diss}$ (μmol $l^{-1}$) | 2.2 | 0.4 | 5.2 | 15.0 |
| Salinity (PSU) | 6.6* | 6.0* | 5.7* | 6.1* |
| Temperature (°C) | 7.4* | 1.1* | 4.5* | 3.1* |
| pH | 6.5 | – | 7.2 | 7.1 |
| $E_h$ (mV) | 439 | 386 | 328 | 384 |

* Values determined ca. 1 m above the sediment

Figure 2 presents concentrations of dissolved species ($PO_4$-P, $NO_3$-N, $NH_4$-N, $SiO_4$-Si, Fe, and Mn) in the sediment-water interface at AS2, BISA1, and BZ1. All concentrations increased with sediment depth, though $NO_3$-N had subsurface peak values. $PO_4$-P and $NH_4$-N were lowest at AS2, whereas $SiO_4$-Si was fairly similar among the sites. $Mn_{diss}$ was also lowest at AS2, while at this site, $Fe_{diss}$ was highest. At BISA1, $Fe_{diss}$ was low and stable with respect to sediment depth.

Deep pore water profiles of $PO_4$-P, $Fe_{diss}$, and $Mn_{diss}$ at sites C63, BISA1, and BZ1 are plotted with solid phase P data in Fig. 3. Generally, $PO_4$-P increased with sediment depth and was highest at BISA1. $Fe_{diss}$ was low and stable at BISA1 and BZ1, while at C63 it had a peak value at 3 cm depth. $Mn_{diss}$ increased down to about 2 cm depth, below which it decreased.

### Sediments

Figure 4 and Table 3 present the elemental compositions of the sediments. Only $TP_{sed}$, $TC_{sed}$, and SAR are available for sites C55, C74, and C6. At these sites,

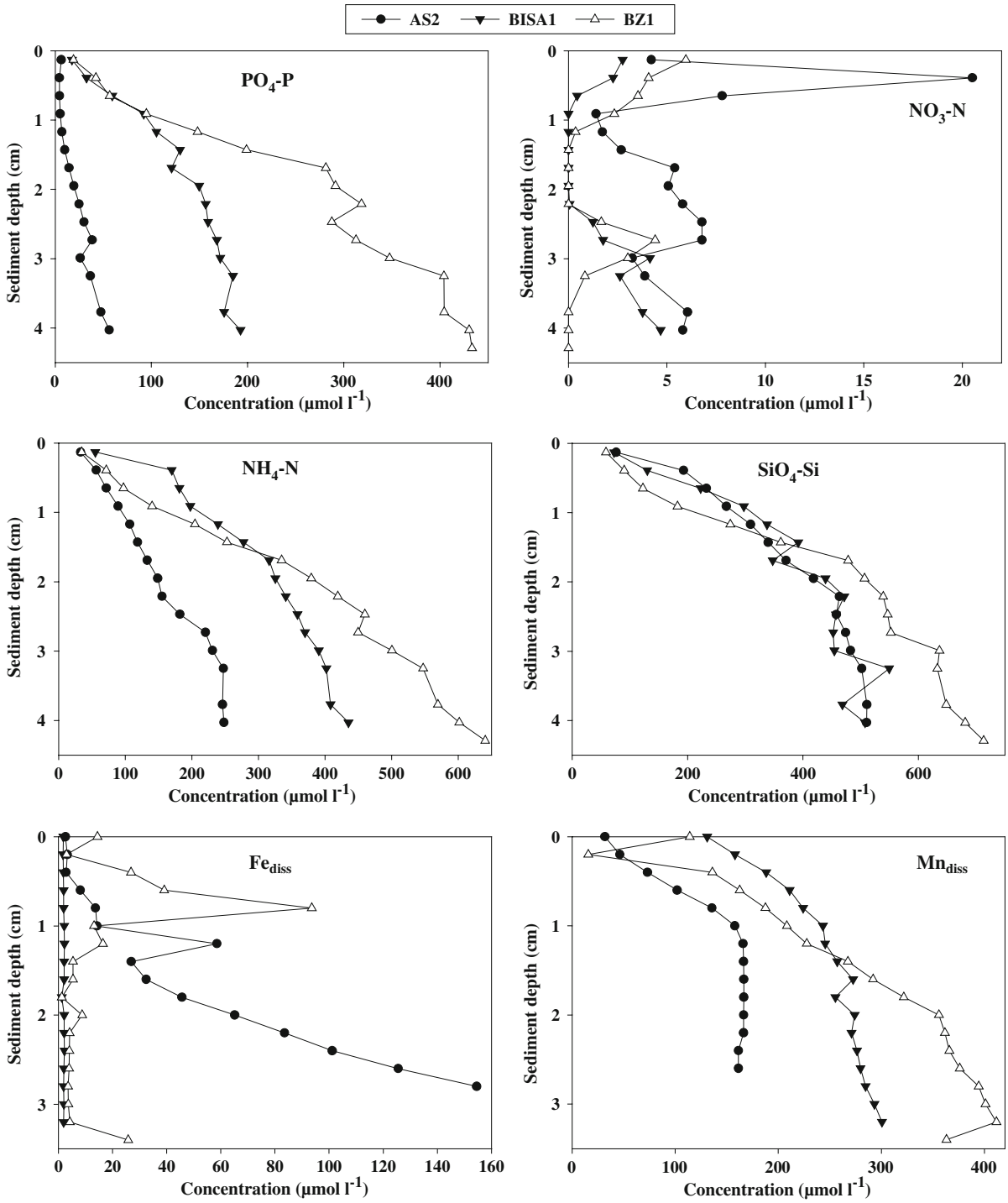


**Fig. 2** Dissolved $PO_4$-P, $NO_3$-N, $NH_4$-N, Fe, and Mn in the sediment pore water. The *y*-axis represents sediment depth in cm. The *x*-axis represents concentration in µmol $l^{-1}$

$TP_{sed}$ and $TC_{sed}$ varied from 21.8 to 66.8 and from 1,174 to 8,492 µmol $g^{-1}$ DW, respectively. $TP_{sed}$ was highest in the surface layer at BISA1 and lowest at C63 (Fig. 4). Generally, it decreased with sediment depth, mostly just below the surface. Among the main sites, the easternmost (BISA1 and BZ1) were clearly highest

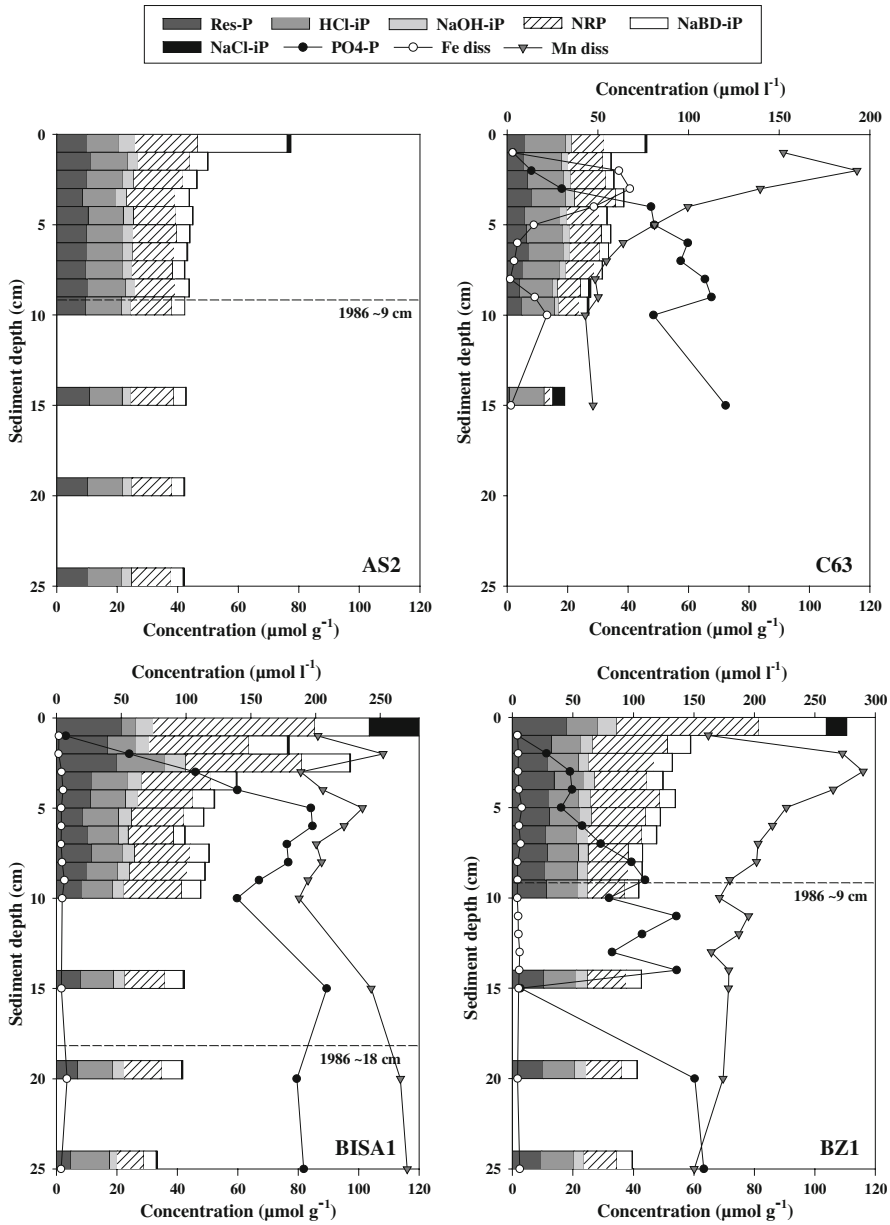


**Fig. 3** Dissolved $PO_4$-P, Fe, and Mn in the deep sediment pore water and vertical distribution of P fractions in sediments. The *y*-axis represents sediment depth in cm. The *x*-axis on top represents concentration of dissolved species in the pore water in μmol $l^{-1}$ and the *x*-axis below represents concentration of P fractions in μmol $g^{-1}$ DW. Differences between replicates were <1.2, <1.2, <1.6, <1.7, and <1.5 μmol P $g^{-1}$ DW for fractions NaCl-iP, NaBD-iP, NaOH-iP, HCl-iP, and Res-P, respectively. The dotted lines show the approximate depth of the $^{137}$Cs maxima (i.e., year 1986)

in $TC_{sed}$ and $TN_{sed}$. Both elements decreased with depth and were lowest at C63. $TS_{sed}$ tended to increase with sediment depth, although it was variable. $TS_{sed}$ was highest at BZ1 and lowest at AS2.

$TFe_{sed}$ was also variable (Table 3), but it mainly increased with depth. Site AS2 was richest and C63 poorest in $TFe_{sed}$. Similarly, $TAl_{sed}$ increased with sediment depth and AS2 was richest and BISA1 was poorest in $TAl_{sed}$. Unlike Fe and Al, $TMn_{sed}$ tended to decrease with sediment depth. It was highest at BZ1, and lowest at C63. In contrast, C63 was richest and BZ1 poorest in $TCa_{sed}$.

The SAR was highest at sites C74 and C6 and lowest at BZ1. The rest of the sites (not determined at C63) had similar SAR values (Table 4). At the main sites, clay (<2 μm) was the predominant particle size fraction (70–74%). However, at C63, the percentage of clay was smaller (55%) and the coarsest size fraction (20–60 μm, 18%) was higher than at other sites. Among the main sites, the redox potential was

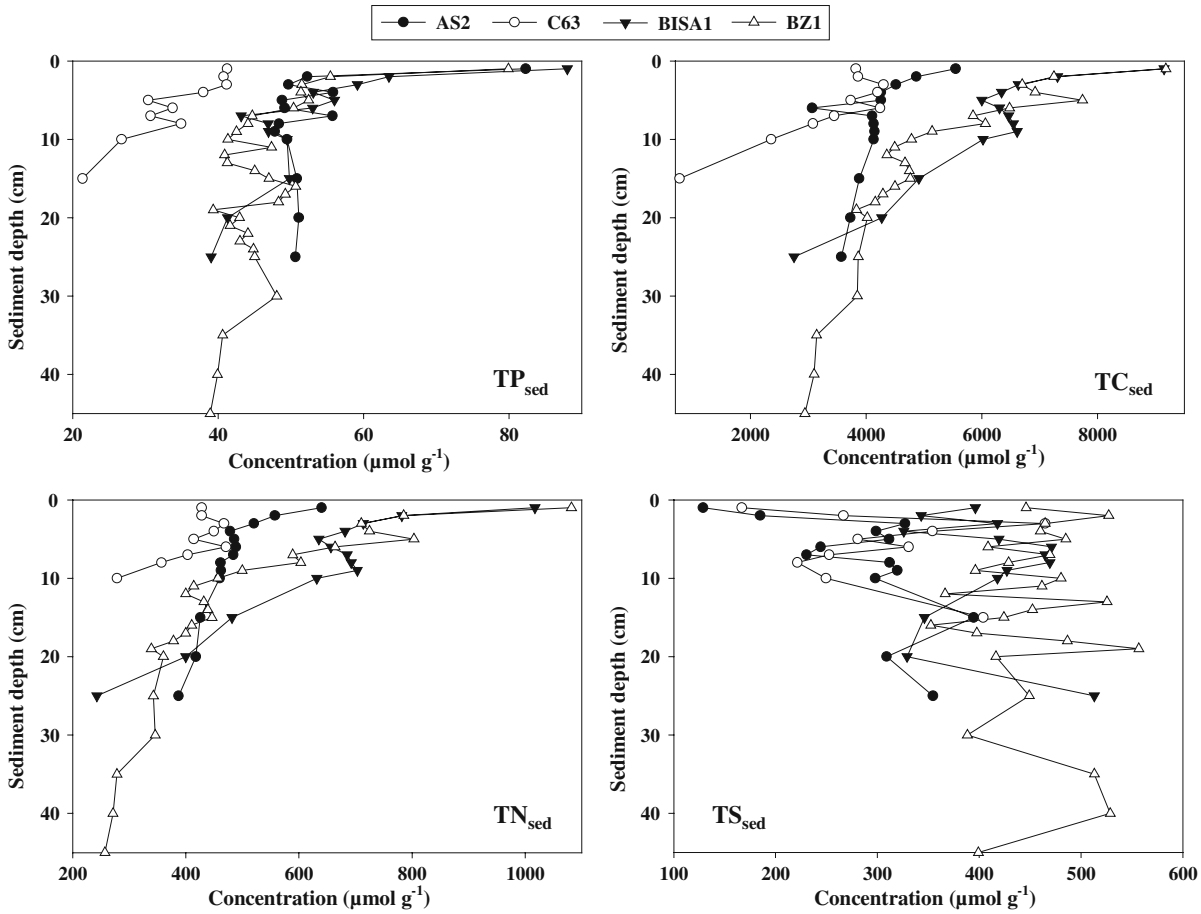


**Fig. 4** Total concentrations of P, C, N, and S in the sediment depth profiles. The *y*-axis represents sediment depth in cm. The *x*-axis represents element concentration in µmol $g^{-1}$ DW

highest at AS2 and lowest at BZ1. It varied between 439 and 328 mV in the near-bottom water and between 432 and −218 mV in the sediment. The redox-potential decreased downwards in the sediment, the drop being strongest within the uppermost 1–2 cm. The pH ranged from 6.5 to 7.2 in the near-bottom water and from 6.7 to 7.3 in the sediment. It was highest at BISA1 and lowest at AS2. It decreased down to 2–3 cm sediment depth.

## P Fractions

$TP_{extr}$ decreased with sediment depth (Fig. 3), especially at BISA1 and BZ1, which were richest in $TP_{extr}$, while C63 was poorest. C63 was also lowest in OP (NRP and Res-P; 45% of $TP_{extr}$), whereas BZ1 was highest (59%). OP dominated only in two depth layers at C63, while at the rest of the sites it dominated in most layers. Immobile P ranged from 12.5 to 42.8 µmol $g^{-1}$ DW, and reactive P from 6.5 to 91.9 µmol $g^{-1}$ DW.

NRP (26–43% of $TP_{extr}$, range 2–53 µmol $g^{-1}$ DW) was the predominant P form at AS2, BISA1, and BZ1 (Fig. 3). At C63, however, HCl-iP dominated, though NaBD-iP was fairly high at the surface. At the other sites, HCl-iP (4–38%; 4.8–13.4 µmol $g^{-1}$ DW) or Res-P (4–28%; 0.8–21.7 µmol $g^{-1}$ DW) were the second most abundant P forms. NaBD-iP (4–38%; 0.8–29.4 µmol $g^{-1}$ DW) was highest at the sediment surface and it sharply decreased with depth. NaBD-iP was also slightly more abundant than NaOH-iP (2–9%; 0.3–6.7 µmol $g^{-1}$ DW) in the deep sediment layers. Concentrations of NaOH-iP and HCl-iP were relatively stable throughout the core depths. NaCl-iP was small, except at the surface at BZ1 and BISA1, and at 15 cm depth at C63 (21% of $TP_{extr}$).

**Table 3** Total concentrations of Fe, Mn, Al, and Ca in sediment depth profiles

| Depth (cm) | AS2 | | | | C63 | | | | BISA1 | | | | BZ1 | | | |
|---|---|---|---|---|---|---|---|---|---|---|---|---|---|---|---|---|
| | Fe | Mn | Al | Ca | Fe | Mn | Al | Ca | Fe | Mn | Al | Ca | Fe | Mn | Al | Ca |
| 1 | 797 | 18.0 | 2,630 | 242 | 567 | 13.2 | 2,268 | 299 | 587 | 39.6 | 1,784 | 249 | 465 | 27.4 | 1,706 | 220 |
| 2 | 821 | 11.9 | 2,872 | 272 | 644 | 11.4 | 2,436 | 289 | 647 | 22.4 | 2,071 | 253 | 769 | 30.5 | 2,182 | 248 |
| 3 | 918 | 13.6 | 2,744 | 243 | 739 | 12.8 | 2,531 | 274 | 724 | 21.5 | 2,117 | 253 | 778 | 32.2 | 2,359 | 241 |
| 4 | 1,006 | 18.2 | 3,196 | 294 | 663 | 12.6 | 2,622 | 284 | 669 | 20.2 | 2,227 | 254 | 790 | 34.5 | 2,238 | 240 |
| 5 | 956 | 17.4 | 2,939 | 268 | 637 | 10.8 | 2,459 | 244 | 868 | 22.8 | 2,759 | 298 | 735 | 38.3 | 2,223 | 229 |
| 6 | 922 | 19.1 | 2,883 | 282 | 672 | 12.8 | 2,648 | 262 | 735 | 21.0 | 2,356 | 268 | 789 | 30.5 | 2,688 | 240 |
| 7 | 965 | 20.2 | 3,356 | 305 | 568 | 11.3 | 2,170 | 252 | 653 | 16.6 | 2,047 | 208 | 809 | 23.2 | 2,428 | 214 |
| 8 | 926 | 17.8 | 3,090 | 269 | 607 | 12.2 | 2,869 | 287 | 700 | 18.8 | 2,088 | 215 | 746 | 23.0 | 2,305 | 202 |
| 9 | 913 | 17.0 | 2,924 | 252 | | | | | 621 | 19.1 | 2,014 | 223 | 770 | 24.1 | 2,497 | 207 |
| 10 | 925 | 18.1 | 3,034 | 260 | 605 | 11.2 | 2,407 | 322 | 768 | 23.8 | 2,471 | 252 | 884 | 25.0 | 2,613 | 216 |
| 11 | | | | | | | | | | | | | 985 | 28.5 | 3,007 | 232 |
| 12 | | | | | | | | | | | | | 785 | 22.7 | 2,664 | 207 |
| 13 | | | | | | | | | | | | | 954 | 25.2 | 2,801 | 201 |
| 14 | | | | | | | | | | | | | 867 | 30.1 | 2,645 | 231 |
| 15 | 1,008 | 18.1 | 3,015 | 255 | 562 | 8.3 | 2,129 | 334 | 764 | 30.1 | 2,607 | 282 | 822 | 33.4 | 2,627 | 218 |
| 16 | | | | | | | | | | | | | 853 | 27.1 | 3,107 | 235 |
| 17 | | | | | | | | | | | | | 927 | 26.1 | 3,153 | 238 |
| 18 | | | | | | | | | | | | | 974 | 24.9 | 2,885 | 238 |
| 19 | | | | | | | | | | | | | 956 | 23.0 | 2,880 | 217 |
| 20 | 952 | 18.2 | 2,692 | 261 | | | | | 693 | 27.8 | 2,340 | 241 | 821 | 21.8 | 3,261 | 214 |
| 21 | | | | | | | | | | | | | 833 | 21.4 | 2,656 | 209 |
| 22 | | | | | | | | | | | | | 914 | 23.2 | 2,577 | 205 |
| 23 | | | | | | | | | | | | | 838 | 22.9 | 2,734 | 214 |
| 24 | | | | | | | | | | | | | 796 | 22.5 | 2,734 | 219 |
| 25 | 997 | 17.6 | 3,012 | 250 | | | | | 735 | 21.4 | 2,304 | 249 | 862 | 22.6 | 2,878 | 228 |
| 30 | | | | | | | | | | | | | 903 | 21.7 | 2,895 | 234 |
| 35 | | | | | | | | | | | | | 1,027 | 18.8 | 2,825 | 225 |
| 40 | | | | | | | | | | | | | 972 | 18.4 | 2,884 | 227 |
| 45 | | | | | | | | | | | | | 835 | 16.0 | 2,838 | 205 |

All concentrations are presented in μmol $g^{-1}$ DW

**Table 4** Sediment accumulation rates (SAR), sedimentation of extractable P, burial fluxes of immobile P, long-term average for minimum annual P efflux, and burial efficiency of total P at different sites

| Site | SAR ($g\ m^{-2}\ year^{-1}$) | Sedimentation of P | | Burial of P | | Long-term average for minimum P efflux | | Burial effic. (%) |
|---|---|---|---|---|---|---|---|---|
| | | ($mmol\ m^{-2}\ year^{-1}$) | ($g\ m^{-2}\ year^{-1}$) | ($mmol\ m^{-2}\ year^{-1}$) | ($g\ m^{-2}\ year^{-1}$) | ($mmol\ m^{-2}\ year^{-1}$) | ($mg\ m^{-2}\ year^{-1}$) | |
| AS2 | 900* | 69.6 | 2.2 | 39.5 | 1.2 | 1.8 | 54.9 | 57 |
| BISA1 | 990 | 123 | 3.8 | 50.9 | 1.6 | 4.0 | 124 | 41 |
| BZ1 | 430 | 47.5 | 1.5 | 22.6 | 0.7 | 1.4 | 42.9 | 48 |
| C55 | 859 | 41.3** | 1.3** | – | – | – | – | – |
| C74 | 1,479 | 98.8** | 3.1** | – | – | – | – | – |
| C6 | 1,438 | 86.9** | 2.7** | – | – | – | – | – |

* SAR value for site AS2 is presented in Mattila et al. (2006); ** Calculated from $TP_{sed}$ at the sediment surface

Table 4 presents sedimentation and burial of P, long-term average of minimum annual P efflux, and burial efficiency of total P in the sediment surface at AS2, BISA1, and BZ1. These variables are not available for the rest of the sites (due to the lack of SAR values or P fractionation results). P sedimentation was highest at BISA1 and lowest at C55. Site BISA1 also had the lowest burial efficiency of total P and highest P efflux. Many of the variables determined in the surface sediment and near-bottom water seemed to reflect $TC_{sed}$. Variables with the closest linear relationship to $TC_{sed}$ (i.e., those with $R^2 > 0.75$ as plotted against $TC_{sed}$) are presented in Fig. 5.

*Total elements in extracts*

Fe extracted in NaBD decreased with sediment depth (Table 5), while in NaOH extract, Fe concentrations were very variable. Site C63 was the poorest in extracted Fe. Al concentrations were high in NaOH and NaOH extracted most Al at BISA1 and BZ1. Mn was extracted mainly in NaBD. Sites BISA1 and BZ1

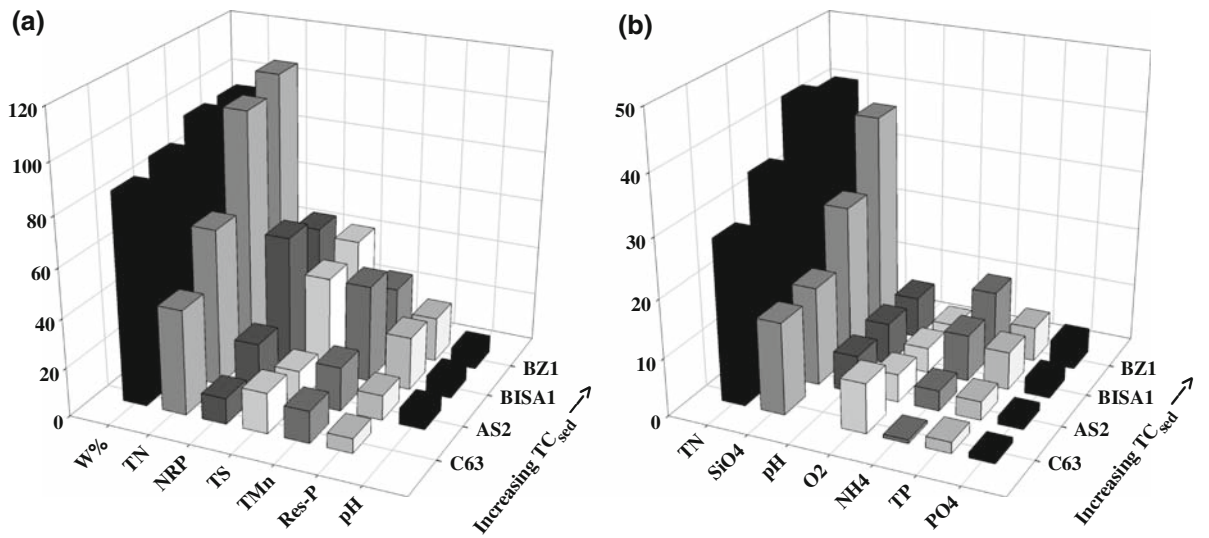


**Fig. 5** Surface sediment (**a**) and near-bottom water (**b**) variables when plotted in order of increasing $TC_{sed}$ concentration in the topmost 1-cm layer at the main study sites. These parameters had $R^2 > 0.75$ when plotted against $TC_{sed}$ at each site. The unit for sediment variables (**a**) is $\mu mol\ g^{-1}$ DW, except $\times 10^{-1}$ $\mu mol\ g^{-1}$ DW for $TN_{sed}$ and $TS_{sed}$. Water content (W%) is expressed in percentages. The unit for near-bottom water variables (**b**) is $\mu mol\ l^{-1}$, except $ml\ l^{-1}$ for $O_2$

**Table 5** Total concentrations of dissolved elements extracted along with P in NaBD and in NaOH

| Depth (cm) | NaBD | | | | | | NaOH | | | | | |
|---|---|---|---|---|---|---|---|---|---|---|---|---|
| | Mg | Si | Al | Ca | Mn | Fe | Mg | Si | Al | Ca | Mn | Fe |
| *AS2* | | | | | | | | | | | | |
| 1 | – | 8.8 | 1.0 | 8.6 | 6.5 | 63.2 | – | 562 | 64.7 | 0.2 | 0.2 | 11.5 |
| 2 | – | 6.2 | 1.1 | 5.0 | 0.9 | 45.9 | – | 555 | 63.0 | 0 | 0.1 | 4.0 |
| 3 | – | 8.2 | 1.5 | 7.3 | 2.4 | 66.3 | – | 528 | 70.2 | 0 | 0.1 | 6.9 |
| 4 | – | 8.0 | 1.0 | 6.9 | 3.0 | 71.3 | – | 517 | 74.6 | 0.1 | 0.2 | 13.9 |
| 5 | 6.2 | 10.2 | 0.8 | 10.9 | 5.1 | 24.7 | 0.2 | 434 | 54.5 | 0.2 | 0.1 | 2.4 |
| 6 | 6.6 | 9.5 | 0.7 | 11.1 | 5.6 | 25.6 | 0 | 433 | 54.5 | 0 | 0.1 | 2.2 |
| 7 | 7.5 | 8.7 | 0.9 | 12.1 | 5.8 | 20.2 | 0 | 430 | 53.2 | 0.2 | 0.1 | 1.9 |
| 8 | 5.6 | 9.0 | 0.5 | 9.5 | 5.5 | 29.6 | 0.6 | 445 | 57.5 | 0 | 0.1 | 3.0 |
| 9 | 5.8 | 11.6 | 0.3 | 9.4 | 5.4 | 20.4 | 0.4 | 492 | 61.1 | 0 | 0.1 | 1.7 |
| 10 | 3.0 | 8.8 | 0.2 | 6.2 | 3.1 | 23.1 | 0.9 | 468 | 61.5 | 0 | 0.1 | 3.9 |
| 15 | 6.0 | 10.8 | 0.4 | 9.1 | 4.1 | 19.3 | 1.6 | 297 | 59.1 | 0 | 0.1 | 4.9 |
| 20 | 6.8 | 9.9 | 0.8 | 10.1 | 3.8 | 14.5 | 1.0 | 221 | 54.2 | 0 | 0.2 | 3.7 |
| 25 | 6.9 | 8.4 | 0.5 | 9.4 | 3.3 | 12.5 | 1.2 | 244 | 55.6 | 0 | 0.2 | 3.5 |
| *C63* | | | | | | | | | | | | |
| 1 | 1.7 | 5.3 | 0.8 | 3.6 | 2.7 | 26.9 | 0.2 | 362 | 39.0 | 0 | 0 | 3.9 |
| 2 | 1.5 | 4.5 | 0.9 | 1.7 | 0.4 | 15.0 | 0.2 | 474 | 42.3 | 0 | 0.1 | 4.2 |
| 3 | 1.9 | 5.1 | 0.9 | 2.1 | 0.5 | 22.4 | 0 | 581 | 51.1 | 0 | 0.1 | 4.5 |
| 4 | 2.5 | 8.8 | 1.1 | 2.8 | 0.5 | 49.3 | 3.6 | 1,100 | 72.2 | 0.2 | 0.3 | 16.2 |
| 5 | 1.8 | 6.4 | 0.8 | 2.8 | 0.4 | 42.1 | 0 | 725 | 51.2 | 0 | 0.1 | 4.0 |
| 6 | 1.5 | 8.0 | 2.4 | 1.3 | 0.2 | 28.0 | 0 | 575 | 50.7 | 0 | 0.1 | 4.5 |
| 7 | 1.3 | 6.3 | 0.5 | 1.7 | 0.2 | 33.4 | 0 | 629 | 48.9 | 0 | 0.1 | 3.1 |
| 8 | 1.3 | 5.6 | 0.7 | 1.7 | 0.2 | 26.2 | 0 | 570 | 46.3 | 0 | 0.2 | 4.9 |
| 9 | 0.9 | 4.6 | 0.5 | 0.9 | 0.1 | 17.7 | 1.0 | 374 | 41.7 | 0 | 0.2 | 6.4 |
| 10 | 1.1 | 4.6 | 0.7 | 0.6 | 0.1 | 19.4 | 0.2 | 334 | 41.3 | 0 | 0.2 | 3.1 |
| 15 | 0.4 | 2.0 | 0.1 | 0.4 | 0.1 | 4.1 | 0 | 32 | 11.7 | 0 | 0 | 2.0 |
| *BISA1* | | | | | | | | | | | | |
| 1 | 14.9 | 13.9 | 1.6 | 13.8 | 14.5 | 39.4 | 0.1 | 1,094 | 60.2 | 0.2 | 0 | 6.2 |
| 2 | 9.7 | 16.6 | 1.6 | 12.0 | 8.0 | 59.9 | 0.4 | 1,083 | 77.0 | 0.3 | 0.1 | 7.9 |
| 3 | 23.8 | 28.9 | 1.3 | 22.7 | 12.2 | 129 | 0.3 | 1,542 | 90.7 | 0.4 | 0 | 9.8 |
| 4 | 6.9 | 17.8 | 1.5 | 8.8 | 7.4 | 69.2 | 0.3 | 1,141 | 88.4 | 0.5 | 0.2 | 13.8 |
| 5 | 7.1 | 17.2 | 1.6 | 8.9 | 7.1 | 62.2 | 0 | 1,031 | 85.2 | 0.3 | 0.1 | 3.7 |
| 6 | 6.4 | 21.7 | 3.1 | 8.6 | 7.1 | 77.4 | 0.1 | 1,038 | 88.7 | 0.3 | 0.1 | 6.1 |
| 7 | 8.6 | 29.6 | 5.7 | 9.0 | 6.2 | 46.6 | 1.3 | 944 | 83.9 | 0.3 | 0.1 | 15.7 |
| 8 | 10.0 | 21.4 | 1.3 | 11.2 | 8.1 | 43.6 | 2.0 | 1,152 | 95.8 | 0.5 | 0.2 | 20.9 |
| 9 | 10.1 | 20.8 | 0.7 | 11.2 | 7.8 | 60.6 | 2.8 | 1,245 | 98.9 | 0.4 | 0.2 | 24.0 |
| 10 | 9.5 | 21.2 | 0.5 | 10.4 | 7.6 | 73.4 | 2.5 | 1,394 | 101 | 0.6 | 0.3 | 28.4 |
| 15 | 5.6 | 11.6 | 1.1 | 8.1 | 9.7 | 32.1 | 1.5 | 907 | 106 | 0.1 | 0.2 | 10.3 |
| 20 | 4.9 | 9.6 | 0.7 | 7.9 | 11.2 | 34.5 | 1.1 | 659 | 94.6 | 0.1 | 0.3 | 8.4 |
| 25 | 2.7 | 5.9 | 0.4 | 4.4 | 6.5 | 28.2 | 1.8 | 412 | 66.7 | 0.2 | 0.2 | 9.1 |
| *BZ1* | | | | | | | | | | | | |
| 1 | 20.1 | 15.6 | 1.4 | 19.0 | 12.0 | 91.1 | 2.2 | 1,506 | 106 | 0.8 | 0.4 | 29.1 |
| 2 | 8.6 | 17.7 | 1.3 | 10.5 | 8.6 | 85.0 | 0.8 | 1,278 | 98.1 | 0.2 | 0.2 | 17.4 |

**Table 5** continued

| Depth (cm) | NaBD | | | | | | NaOH | | | | | |
|---|---|---|---|---|---|---|---|---|---|---|---|---|
| | Mg | Si | Al | Ca | Mn | Fe | Mg | Si | Al | Ca | Mn | Fe |
| 3 | 9.0 | 19.2 | 0.9 | 7.6 | 12.6 | 105 | 0.9 | 1,321 | 101 | 0.7 | 0.2 | 13.4 |
| 4 | 8.2 | 14.5 | 2.0 | 12.0 | 11.4 | 56.4 | 1.0 | 1,185 | 99.8 | 0.3 | 0.3 | 15.0 |
| 5 | 6.3 | 15.0 | 1.1 | 9.6 | 9.1 | 50.5 | 2.7 | 1,372 | 106 | 1.1 | 0.5 | 36.1 |
| 6 | 7.4 | 14.4 | 1.1 | 9.6 | 8.8 | 45.2 | 0.7 | 1,296 | 104 | 0.2 | 0.2 | 10.7 |
| 7 | 8.9 | 17.5 | 0.9 | 11.3 | 9.3 | 92.0 | 0.8 | 1,420 | 114 | 0.3 | 0.2 | 13.4 |
| 8 | 7.2 | 12.6 | 1.0 | 9.1 | 8.6 | 54.0 | 0 | 1,228 | 103 | 0 | 0.1 | 2.7 |
| 9 | 6.7 | 12.9 | 1.3 | 9.1 | 9.2 | 51.3 | 0.1 | 1,136 | 105 | 0 | 0.2 | 4.0 |
| 10 | 5.1 | 10.8 | 1.3 | 6.9 | 7.2 | 39.2 | 0 | 1,057 | 95.9 | 0 | 0.1 | 2.5 |
| 15 | 4.3 | 9.8 | 1.1 | 6.3 | 6.5 | 35.2 | 0.4 | 1,204 | 105 | 0.1 | 0.2 | 5.6 |
| 20 | 5.1 | 10.9 | 2.4 | 6.5 | 5.3 | 38.0 | 0 | 1,213 | 97.1 | 0 | 0.2 | 4.0 |
| 25 | 4.8 | 11.0 | 1.2 | 6.8 | 6.1 | 31.9 | 0 | 1,148 | 93.9 | 0 | 0.2 | 4.6 |

All concentrations are presented as μmol $g^{-1}$DW

Maximum concentration range for Mg, Si, Al, Ca, Mn, and Fe, respectively, of triplicate or duplicate samples—NaBD: <9.3, <26.3, <9.6, <8.7, <2.7, and <23.1; NaOH: <7.3, <231, <29.4, <0.7, <0.3, and <21.7

–, Concentration of the element not determined

0, Concentration below detection limit or <0.05 μmol $g^{-1}$ DW

were the richest in Si, which was mostly extracted by NaOH.

### Statistical analyses

For mixed model analysis, the results obtained from different depth layers were pooled and averaged into five age classes on the basis of $^{137}$Cs dating and by assuming a constant SAR over time. This was necessary to keep the number of variables at each site low enough to run the model. P fractions other than NaCl-iP were related to these age classes, i.e. time. $TP_{sed}$ and OP were also related to time. A summary of the other statistically significant relationships between P fractions and elements in sediments and in the two extracts is presented in Table 6.

## Discussion

### Sediment properties

Sediment accumulation was rapid at all the sites (Table 4). Site C63, however, was affected by transportation. Although SAR was not determined,

**Table 6** Summary of significant relationships between different P fractions, sediment parameters, and other elements in extracts

| Dependent variable | Statistically significant relationship with |
|---|---|
| NaCl-iP | $TCa_{sed}$, NaBD-iP |
| NaBD-iP | $TP_{sed}$, $TC_{sed}$, $TFe_{sed}$, $TCa_{sed}$, NaCl-iP, NaBD-extr. Fe, Mg, Ca |
| NRP | $TN_{sed}$, $TS_{sed}$, $TCa_{sed}$, NaOH-iP, HCl-iP, NaBD-extr. Fe |
| NaOH-iP | $TP_{sed}$, $TFe_{sed}$, NaBD-iP, NRP |
| HCl-iP | $TCa_{sed}$, NaBD-iP, NaOH-iP, NaOH-extr. Fe, Si, Al, Mg |
| Res-P | $TFe_{sed}$ |
| Total OP | $TP_{sed}$, $TC_{sed}$, $TN_{sed}$, $TS_{sed}$, $TCa_{sed}$, NRP, Res-P |
| $TP_{extr}$ | $TC_{sed}$, $TN_{sed}$, $TS_{sed}$, $TFe_{sed}$, $TCa_{sed}$, NaOH-iP, NRP, Res-P |

Sed (as a subscript), content in the sediment

this was apparent because the bottom sediment was hard below 15 cm depth. Moreover, at C63 the sediment had the coarsest texture, i.e., this site was the poorest in the clay size fraction. The relatively low SAR at BZ1 (Table 4), in spite of a $^{137}Cs$ peak value at 9 cm depth, was probably the result of high OM and water content in the surface sediment. Unlike in GoF sediments from sites with a water depth of >60 m (Lukkari et al., submitted), in shallow coastal areas, sedimentation of P did not closely follow SAR. Site BISA1 received the most P, followed by C74, although sedimentation was faster at C74. Similarly, BZ1 received more P than C55, although the SAR for C55 was twice that of BZ1. This difference in SAR and P accumulation between open sea and shallow coastal area probably reflects the calmer conditions that allow sedimentation of P-rich fine particles in deeper basins than at coastal sites.

$TC_{sed}$ was lowest at the site most strongly affected by transportation and with the coarsest texture (C63) because light and fine particulate OM is easily resuspended. The good oxygenation of the sediment may also have enhanced mineralization. $TC_{sed}$ was highest at the easternmost sites and (excluding C63) decreased westwards, being lowest in the AS. Carman (1998) and Lukkari et al. (submitted) also reported an increasing trend in $TC_{sed}$ towards the inner bay, which is related to the heavy nutrient load and the inflow of the Neva River at the eastern end of the GoF. $TC_{sed}$ seemed to affect several other sediment properties. Figure 5a illustrates the increasing trends of some variables for surface sediments, when the main sites were organized in order of increasing $TC_{sed}$.

Among the main sites, AS2 was richest in sediment Fe and Al (Table 3). This site is located close to a bay that receives high amounts of river-transported clayey material (Lukkari et al. 2008). Material eroded from clayey soils of southern Finland is rich in poorly crystallized Fe and Al oxides effective in P binding (Hartikainen 1979; Peltovuori 2006). Total concentrations of Fe and Al can be indicative of their presence. This explains why $TP_{sed}$ was high at AS2 (Fig. 3), despite the fact that for the rest of the sites, it seemed to follow OM content, being high at the eastern coast (BISA1 and BZ1) and low at C63. Low $TP_{extr}$ at C63 can also result from the coarser texture there, as poorly crystallized oxides of Fe and Al are enriched in the fine particulate fraction. High alkali-soluble Al at BISA1 and BZ1 may be related to the presence of organometallic compounds (Schnitzer 1969).

The decrease of $TP_{sed}$, $TC_{sed}$, and $TN_{sed}$ with sediment depth (Fig. 4) reflect degradation of OM (e.g. Kemp 1971). $TP_{sed}$ also decreases because Fe–P is released in reduced layers and enriched in oxic surface (Mortimer 1971). The increasing trends in concentrations of Fe, Al, and $TS_{sed}$ with depth (Table 3) indicate changes in mineral composition. In OM-rich sediments, the decrease in $TS_{sed}$ in the surface layer can be related to degradation of OM containing S, while the subsurface increase suggests formation of ferro-sulfides (Berner 1970; Jørgensen 1977). Moreover, at site BISA1, the elevated pH, reduced conditions, and presence of white bacterial growth (possibly sulfide-oxidizing *Beggiatoa* sp.; Jørgensen 1977), indicate sulfate reduction (Martens and Goldhaber 1978; Caraco et al. 1989). Also, dark grey and black laminas in reduced OM-rich sediments coinciding with high $TS_{sed}$ suggest the presence of ferro-sulfides and pyrite (Berner 1970) and, thus, diminished capacity for P binding because of Fe removal (Mortimer 1971; Krom and Berner 1980; Caraco et al. 1989; Anschutz et al. 1998). Near-bottom water at BISA1 and BZ1 was oxic (Table 2) but, evidently, the high OM content consumed $O_2$ from the sediment surface, creating reducing conditions. Reduced OM-rich sediments are common in the shallow, seasonally hypoxic basins of the AS and the northern coast of the GoF (Virtasalo et al. 2005; Vallius 2006; Kotilainen et al. 2007).

## Vertical and spatial distribution of P

The decrease in $TP_{extr}$ (Fig. 3) with depth was strongest at the eastern coast, which was high in OM and OP, and it seemed to be related to degradation of OP. At C63, on the other hand, lower $TP_{extr}$ and OP suggested removal of fine particles. Sediment cores at the main sites had unclearly laminated sedimentary units, indicating that benthic fauna affected distribution of elements.

### *Immobile P*

Immobile P, which consists of P bound to Al-oxides (NaOH-iP), apatite-P (HCl-iP), and refractory OP

(Res-P), is supposed to be buried and removed from the nutrient cycle. In contrast, reactive P, which includes soluble or loosely-bound P (NaCl-iP), redox-sensitive P (mainly Fe-bound; NaBD-iP), and labile OP (NRP), may be available for aquatic organisms or become so due to biogeochemical processes. However, some reactive P is present in deep sediment layers and becomes buried (Jensen and Thamdrup 1993; Lukkari et al. 2008, submitted). In the present study, the portion of immobile P (26–66% of $TP_{extr}$) was lowest at OM-rich and highest in OM-poor sites. Immobile P forms were fairly stable with sediment depth and they predominated in deep layers.

P bound to oxides of non-reducible metals (NaOH-iP) was one of the most stable P form. Its proportion of $TP_{extr}$ in these coastal sediments was less than 10%, i.e., smaller than in nearby estuary sediments but higher than in the central GoF (Lukkari et al. 2008, submitted). This suggests that this P form has its origin in river-transported clayey material. Clay particles often have metal oxide coatings, effective in binding P. In addition to displacement of $PO_4$-P with hydroxyl ions, alkaline extraction dissolves OM. Although part of the Al (and Fe) released in alkali extraction may originate from disrupted oxide structures, their abundance in OM-rich sediments from the eastern coast (Table 5) suggests the presence of organometallic compounds. Schnitzer (1969) showed that Al and Fe, which form complexes with humic acids, bind P and, for example, Williams et al. (1971b) and Paludan and Jensen (1995) found that a part of sediment OP is associated with Al.

The fractionation scheme used does not separate detrital and authigenic apatite (Ruttenberg 1992), but it is expected that most of the apatite-P (HCl-iP) in these coastal $CaCO_3$-poor sediments was of terrestrial origin. Furthermore, Virtasalo and Kotilainen (2008) showed that in the surface sediments of the AS, authigenic apatite-P was about six times lower than detrital apatite-P. Detrital apatite-P is a fairly inert P form, which can also be concluded from the more or less stable vertical distribution of apatite-P fraction (Fig. 3) (Jensen and Thamdrup 1993; Lukkari et al. 2008). Apatite-P was the predominant P form at the site most affected by transportation (C63) as also found by Williams et al. (1976) in lake sediments. Site C63 was also coarsest in texture, lowest in OP (and OM), and highest in $TCa_{sed}$ (Table 3). In contrast, apatite-P formed a smaller proportion of $TP_{extr}$ on the OP-rich eastern coast, which was higher in clayey material and poorer in $TCa_{sed}$ (BISA1 and BZ1). This spatial difference between apatite-P and OP was probably responsible for the statistically significant relationship between OP and $TCa_{sed}$ (Table 6).

The residual P fraction is supposed to represent refractory OP, although it contains some slowly degradable as well as inorganic P as well (Ruttenberg 1992; Lopez 2004). Residual P was amongst the three most abundant P forms at all coastal sites. It was most abundant in the OM-rich sediments on the eastern coast, while the transportation area (C63) was poorest in refractory OP. Residual P slightly decreased with sediment depth at the eastern sites. This may be attributable to the presence of slowly degradable OP compounds (Reitzel et al. 2007) or increased sedimentation of OM in the coastal area. In fact, Vaalgamaa and Conley (2008) reported that sedimentation has increased during the past decades in small shallow bays in the northern GoF. In the coastal sediments examined in the present study, Fe content was the only sediment variable to which residual P was statistically related (Table 6). A similar relationship was found previously by Williams et al. (1976), who suggested that it may result from indirect relations via other sediment variables (OC and clay contents). However, it may also be related to the presence of organometallic complexes stable against degradation (Schnitzer 1969). Although the relationship between residual P and $TC_{sed}$ was not statistically significant, residual P increased with increasing $TC_{sed}$ content (Fig. 5a).

*Reactive P*

Reactive P formed 34–74% of $TP_{extr}$ in coastal sediments. In fact, in the surface sediments from the eastern coast, reactive P was highest, as determined in our previous studies, in the northeastern BS (Lukkari et al. 2008, submitted). At the easternmost sites (i.e., closest to the inner bay), the concentration of reactive P strongly decreased with sediment depth and predominated over immobile P in deeper sediment layers than at the other sites.

Usually, pore water or loosely-bound P (NaCl-iP) forms only 1–2% of $TP_{extr}$ (e.g., Jensen et al. 1995; Lukkari et al. 2008, submitted). However, the sites on the eastern coast were exceptional: in the surface

layer at BISA1, this P form, which is readily available to bacteria and algae (Van Eck 1982), formed 17% of $TP_{extr}$ and, at BZ1, the percentage was 6% (Fig. 3). The abundance of the loosely-bound P reflects a lack of available sorption sites for $PO_4$-P. A lack of sorption sites can result from highly occupied sorption surfaces, reducing conditions in the sediment (as was the case at BISA1 with its high positive incubation-derived $PO_4$-P flux; Table 2), or from anion competition (e.g., with silicate (Fig. 2) and organic acids; Hingston et al. 1967; Koski-Vähälä et al. 2001).

The highest concentrations of P bound to Fe oxyhydroxides (NaBD-iP) in the topmost 0–1 cm layers (Fig. 3) was expected, since in muddy sediments, the oxygenated layer is usually restricted to several millimetres depth (Mortimer 1971; Conley et al. 1997). In agreement with the assumed binding form, this P fraction was statistically significantly related to reductant-soluble Fe and Mn (Table 6). However, it has been found that some Fe-bound P can be buried with sediment due to incomplete Fe reduction (Berner et al. 1993; Slomp et al. 1996b; Hyacinthe and Van Cappellen 2004). Coastal sediments in this study also buried Fe-bound P (Fig. 3), though considerably less than sediments in the nearby shallow estuaries (Lukkari et al. 2008). One reason for this was probably the slower sedimentation rate in the coastal areas. Fe-bound P was higher in the AS (AS2) than at site C63, even though the transportation-affected site had better $O_2$ conditions. AS2 was also higher in reductant-soluble Fe as well as in total sediment Fe; thus, it is likely that the higher Fe-bound P at AS2 resulted from the fine particulate Fe-rich material this site received from the estuary. Although site AS2 was higher in sediment Fe than the OM-rich sediments on the eastern coast, surface sediments at the eastern sites were fairly high in reductant-soluble Fe. It is possible that an abundance of $PO_4$-P, $SiO_4$-Si, and organic anions (Shukla et al. 1971; Slomp et al. 1996b) as well as alternating oxic–anoxic conditions (Coey et al. 1974) retard crystallization of poorly crystallized Fe (and Al) oxides, maintaining their high sorption capacity. All these coastal sites had $O_2$ concentrations higher than 2 ml $l^{-1}$ in the near-bottom waters. However, at BISA1, the reducing conditions and the high loosely-bound P at the sediment surface indicate dissolution of Fe oxides.

Labile OP (NRP) was the predominant P form at the oxic coastal areas studied, except for the apatite-P-rich site (C63), which located in transportation area. This P fraction contains e.g., orthophosphate monoesters (e.g., inositol phosphates) and diesters (DNA, phospholipids) as well as polyphosphates and pyrophosphates that are inorganic storage compounds and degradation products (Hupfer et al. 2004; Ahlgren et al. 2005; Reitzel et al. 2006). Unlike total OP (i.e., Res-P and NRP), labile OP did not have statistically significant relationship with $TC_{sed}$ (Table 6). However, it had statistically significant relationship with $TN_{sed}$, and it was more abundant at the OM-rich sites (Fig. 5a). The degradation rate of labile OP can be coarsely evaluated based on its half-life ($T_{½}$) in the sediment (Ahlgren et al. 2005). $T_{½}$ for NRP (determined by exponential fitting of concentrations versus sediment age, $R^2 > 0.7$) was 36 years in the AS (AS2), while it was only 6 years at the OM-rich eastern coast. One explanation for faster degradation of OP at the eastern sites may be poorer $O_2$ conditions and, consequently, release of OP bound to particle surfaces (Suzumura and Kamatani 1995; Celi et al. 1999). In the sediment surface layers, the ratios of OC and OP, which characterize OM (Ruttenberg and Goñi 1997), were lower at the two eastern sites, BISA1 (122) and BZ1 (141), than at C63 (229) and AS2 (180). This suggests that OM at the eastern sites contained less material of terrestrial origin than OM on the western coast, which is congruent with the shorter $T_{½}$ of labile OP at the eastern coast sites. This probably reflects the higher P load and productivity in the eastern GoF (Conley et al. 1997). As in surface sediments in the central GoF (Lukkari et al., submitted), the OC:OP ratio and OC:ON ratio (8.5–9.0) exceeded the Redfield ratio (Redfield et al. 1963). This is typical for the BS and indicates OM loading from the large drainage area and enrichment of deposited material with C (Carman 1998; Edlund and Carman 2001; Stepanauskas et al. 2002).

## Dissolved species in the sediment-water interface

The inverse relationship between near-bottom water $O_2$ and $PO_4$-P (Table 2) is in agreement with the theory of more efficient P binding in oxic conditions (Einsele 1936, 1938; Mortimer 1941, 1942). The highest near-bottom water $PO_4$-P (BZ1) also coincided with the steepest concentration gradient of

$PO_4$-P in the sediment-water interface (Fig. 2). However, the incubation-derived $PO_4$-P flux (Table 2) was clearly highest at the site richest in OP (BISA1; Fig. 3). Thus, a part of the $PO_4$-P probably originated in easily degradable OP. This conclusion is supported by the high $NH_4$-N at BISA1, indicating OM degradation (Martens and Goldhaber 1978; Kamp-Nielsen 1992; Slomp et al. 1996b). OP, $TC_{sed}$, and $NH_4$-N were also high at BZ1, where the incubation-derived $PO_4$-P flux was five times lower than at BISA1, probably because of more reduced sediment surface at BISA1. Moreover, BZ1 was higher in $NO_3$-N in the near-bottom water (Table 2) and in the sediment-water interface (Fig. 2) than BISA1. This suggests that in the surface layer at BZ1, Fe was more likely present as Fe oxyhydroxides, which are able to retain P. In fact, reductant-soluble Fe was higher at BZ1 than at BISA1 (Table 5). A peak value for pore water $Fe_{diss}$ at ca. 1-cm depth at BZ1 (Fig. 2) may explain the diffusion of $Fe_{diss}$ into the near-bottom water. At BISA1, in contrast, reduced conditions and low $Fe_{diss}$ in the sediment-water interface indicate that $Fe_{diss}$ had diffused out from the sediment or was incorporated into ferro-sulfides (Berner 1970), as suggested above. Despite the oxidized surface sediment, the incubation-derived $PO_4$-P flux was positive and near-bottom water $Fe_{diss}$ was fairly high at AS2. This may be related to the activity of benthic animals (e.g. Petr 1977; Hietanen et al. 2007), a suggestion that is supported by the partly mixed laminas. Similarly, Conley et al. (1997) reported high $PO_4$-P fluxes in the GoF despite oxic near-bottom water.

Silicate anion is bound to oxide surfaces with a similar mechanism than $PO_4$-P and it competes with $PO_4$-P for sorption sites (Hingston et al. 1967; Ryden et al. 1987; Koski-Vähälä et al. 2001). Although the gradients of $SiO_4$-Si in the sediment-water interface were similar at AS2, BISA1, and BZ1 (Fig. 2), the sites on the eastern coast were higher in $SiO_4$-Si in the near-bottom water (Table 2). This may be related to their higher biogenic Si content, as suggested by high alkali-extractable Si (Table 5). Moreover, scanning electron microscope images revealed an abundance of biogenic silica (mostly diatom remnants) in surface sediment in the eastern GoF (Vallius 1999). At these coastal areas, many parameters in the near-bottom water increased with increasing sediment TC, while the opposite was found for $O_2$ (Fig. 5b). High amounts of OM support active mineralization and other biogeochemical processes that are reflected in the chemistry of the near-bottom water.

## Burial and release of sediment P in the shallow coastal sediments

Reactive P forms buried in deep sediment layers were taken into account when calculating the burial flux and in evaluating the minimum annual P efflux determined on the basis of the solid phase data (Table 4) (Lukkari et al. 2008, submitted). The $TP_{extr}$ of the sediment depth layer deposited in 1986 (i.e., the one with $^{137}Cs$ peak value) was used as the background level. Among the main sampling sites, BISA1, which had the fastest sediment accumulation and P sedimentation rates, also had the highest burial of P (Table 4). However, because this same site, rich in OM and OP, had the lowest burial efficiency for total P in the sediment surface, it also clearly had the highest P efflux when calculated as an annual average since 1986 (Table 4). At BISA1, labile OP seemed to be the P form mostly responsible for the long-term P efflux. Furthermore, the reduced sediment surface restricted the capture of mineralization-released P by Fe oxyhydroxides. Although the chemical composition of sediment P at the other OM-rich site, BZ1, was similar to that at BISA1, the long-term efflux of P at BZ1 was even lower than at the site located in the Fe-rich AS (AS2). The explanation for this seems to be the slower sedimentation and accumulation of P at BZ1. The best burial efficiency for total P in the AS is related to lower OP and abundance of Fe-compounds and their ability to retain soluble P diffusing upwards into the oxic surface layer (Fig. 3).

The chemical characterization of sediment P suggests that, on average, shallow coastal sediments in the AS and in the GoF will bury 49% of total P in the sediment surface layer, while the rest will be released back into the water column with time. Generally, in coastal sediments, sedimentation and burial of P was lower than in nearby estuaries, but higher than in the hypoxic central GoF (Lukkari et al. 2008, submitted). Burial of P at the study sites was also slightly higher than reported for other shallow coastal areas in the BS, e.g., in the Gulf of Riga (Carman et al. 1996) and Aarhus Bay (Jensen et al. 1995). However, at the two coastal sites in the eastern GoF, the burial efficiency of sediment P was lowest found in the studies in the

northeastern BS (Lukkari et al., submitted). This suggests that shallow coastal areas high in OM and OP that occasionally suffer from $O_2$ depletion release a large part of their accumulated sediment P in the long run. Calculation of long-term average values for minimum annual P efflux (Table 4), based on the loss of reactive P from the sediment between year 1986 and the sampling year, assumes that (1) all reactive P lost was released from the sediment to the water column (2) the SAR was constant, and (3) the composition of deposited material remained constant. These estimates suggest that, in these coastal sediments, the average value for minimum annual P release from sediment reserves ranges from 42.9 (at the AS) to 124 kg $km^{-2}$ (at the eastern GoF; Table 4). It is noteworthy that this is higher than similarly determined values for P in the hypoxic sediments in the central GoF (1.3–46.0 kg $km^{-2}$ $year^{-1}$; Lukkari et al., submitted). Relevant to this, Lee et al. (1977) and Boström et al. (1982) suggested that over the long-term, the slow but continuous release of P from shallow lake sediments in aerobic conditions may even exceed that in anaerobic conditions. However, possible increase in SAR (Emeis et al. 2000; Vaalgamaa and Conley 2008) can cause overestimation of P efflux in this study.

Assuming that the burial efficiency of total P at the rest of the coastal sampling sites, C55, C74, and C6, is close to the average value (49%) determined for the sites AS2, BISA1, and BZ1, we can also coarsely estimate P burial and the long-term average of minimum annual P efflux for the former sites. Moreover, combining the long-term P efflux estimates (41.2–115 kg $km^{-2}$ $year^{-1}$) with those presented in Table 4, we can roughly estimate that the shallow coastal areas in the northern GoF (and AS) have annually released about 79 kg P $km^{-2}$ from their sediments during the past 12–18 years. Note, however, that all these minimum estimations are based on information stored in the sediment and do not take into account short-term P release during or right after deposition. Pronounced P release occurs temporarily, for example, after the settling of algal blooms (Williams and Mayer 1972). The incubation-derived flux determinations represent temporal situation and the fluxes have significant spatial and temporal variation. Thus, they are not comparable with the long-term P efflux estimations. According to incubation-derived flux determinations, P efflux is 16.8, 389, and 70.5 mmol $m^{-2}$ $year^{-1}$ for sites AS2, BISA1 and BZ1, respectively. These values represent maximum estimates because the determinations were made in August when the flux is probably high. As pointed out in Lukkari et al. (submitted), using average values during the past 12–18 years probably overestimates the long-term P efflux during years of good $O_2$ conditions and underestimates that when $O_2$ has been depleted from the near-bottom water. Despite the shallowness, $O_2$ depletion is common in the small basins on the northern coast of the GoF and AS because of the patchy bottom topography and thermal stratification during summer. An abundance of laminated sediments indicating poor $O_2$ conditions has also been reported in other coastal areas of the BS (Persson and Jonsson 2000), and their occurrence may even increase in the future as a result of climate change.

## Conclusions

The topographically variable shallow coastal sediments in the AS and northern GoF differed in their content of P and its chemical composition. The site most affected by sediment transportation was poorest in P and it was dominated by immobile apatite-P. In the AS, on the other hand, the Fe-rich oxic sediment surface had abundant P bound to Fe oxyhydroxides. However, sediments in the AS, and especially the OM-rich sediment on the eastern coast of the GoF, were dominated by alkali-extractable, labile OP. An abundance of OP seemed to cause efflux of P from sediment reserves in the long-term. The release of sediment P, including that originating in OP, was most pronounced in sediment that had the most reducing conditions at the surface. For this reason, Fe-compounds were not able to bind P diffusing upwards in the sediment and, instead, the P was released into the water column. Furthermore, the abundance of loosely-bound and pore water P at the same site reflected the lack of available sorption sites for P. P bound to oxides of metals not sensitive to reduction (e.g., Al-oxides) was vertically and spatially the most stable P form. Sediments on the eastern coast high in OM and OP have the lowest burial efficiencies for total P in sediments studied in the northeastern BS so far. In fact, concerning P reserves in the sediment the long-term average of minimum annual P efflux was

generally higher in OM-rich sediments overlain by oxic near-bottom water on the eastern coast than in the poorly oxygenated sediments in the central GoF. Despite the shallow water depth, sediments in sheltered coastal OM-rich sub-basins suffer from seasonal $O_2$ depletion. Moreover, in the future, the surface area of shallow hypoxic basins may even increase in the BS because of climate change. Thus, shallow coastal areas may release a marked part of their P reserves in the long run and their condition should be taken into consideration when trying to resolve the eutrophication problem in the BS as well as in the other eutrophied sea areas. The results suggest that more information is needed on the long-term release of P from coastal sediments and on the role of organic P in P loading.

**Acknowledgments** Financial support was received from the Ministry of the Environment, the Kone Foundation, the Finnish Institute of Marine Research (FIMR), and the Maj and Tor Nessling Foundation. We thank the personnel of the laboratory of the FIMR, the Institute for Environmental Research (University of Jyväskylä), and GTK for chemical determinations. We are indebted to Jyrki Hämäläinen, Kimmo Alvi, and Boris Winterhalter from GTK for help in sediment descriptions and echo sounding during cruises of the r/v Aranda, and Pekka Marttila, Erkki Lintunen and Tiina Helminen for help during cruises of the r/v Kaita. We thank Kalervo Mäkelä and Hannu Haahti from FIMR for the pore water data and the nutrient flux determinations. We thank the personnel of the r/v Aranda for assistance during cruises, and Helinä Hartikainen for comments on the manuscript. Advice on statistical analysis was received from Ville Hallikainen, Risto Häkkinen, Jaakko Heinonen, and Juha Hyvönen from the Finnish Forest Research Institute. This study was part of a project within the SEGUE consortium (Searching for protection tools for the eutrophied GoF—Integrated use of research and modelling tools) carried out at the FIMR, the Finnish Environment Institute, and the University of Helsinki. SEGUE is part of the Baltic Sea Research Programme of the Academy of Finland.

## References

Ahlgren J, Tranvik L, Gogoll A, Waldebäck M, Markides K, Rydin E (2005) Sediment depth attenuation of biogenic phosphorus compounds measured by $^{31}$P NMR. Environ Sci Technol 39:867–872. doi:10.1021/es049590h

Aigars J (2001) Seasonal variations in phosphorus species in the surface sediments of the Gulf of Riga, Baltic Sea. Chemosphere 45:827–834. doi:10.1016/S0045-6535(01)00121-7

Alenius P, Myrberg K, Nekrasov A (1998) The physical oceanography of the Gulf of Finland: a review. Boreal Environ Res 3(2):97–125

Aller RC (1988) Benthic fauna and biogeochemical processes in marine sediments: the role of burrow structures. In: Blackburn TH, Sørensen J (eds) Nitrogen cycling in coastal marine environments. Wiley, Chichester, pp 301–338

Anderson LD, Delaney ML, Faul KL (2001) Carbon to phosphorus ratios in sediments: implications for nutrient cycling. Global Biogeochem Cycles 15(1):65–79. doi:10.1029/2000GB001270

Anschutz P, Zhong S, Sundby B, Mucci A, Gobeil C (1998) Burial efficiency of phosphorus and the geochemistry of iron in continental margin sediments. Limnol Oceanogr 43(1):53–64

Balzer W (1986) Forms of phosphorus and its accumulation in coastal sediments of Kieler Bucht. Ophelia 26:19–35

Bender M, Martin W, Hess J, Sayles F, Ball L, Lambert C (1987) A whole-core squeezer for interfacial pore-water sampling. Limnol Oceanogr 32(6):1214–1225

Berner RA (1970) Sedimentary pyrite formation. Am J Sci 268:1–23

Berner RA, Ruttenberg KC, Ingall ED, Rao J-L (1993) The nature of phosphorus burial in modern marine sediments. In: Wollast R, Mackenzie FT, Chou L (eds) Interactions of C, N, P and S biogeochemical cycles and global change: NATO ASI series, vol 14. Springer, Berlin, pp 365–378

Bonsdorff E, Blomqvist EM, Mattila J, Norkko A (1997) Coastal eutrophication: causes, consequences and perspectives in the Archipelago areas of the northern Baltic Sea. Estuar Coast Shelf Sci 44:63–72

Boström B, Jansson M, Forsberg C (1982) Phosphorus release from lake sediments. Arch Hydrobiol Beih Ergebn Limnol 18:5–59

Caraco NF, Cole JJ, Likens GE (1989) Evidence for sulphate-controlled phosphorus release from sediments of aquatic systems. Nature 341:316–318. doi:10.1038/341316a0

Carman R (1998) Burial pattern of carbon, nitrogen and phosphorus in the soft bottom sediments of the Baltic Sea. Vie Milieu 48(4):229–241

Carman R, Jonsson P (1991) Distribution patterns of different forms of phosphorus in some surficial sediments of the Batic Sea. Chem Geol 90:91–106. doi:10.1016/0009-2541(91)90036-Q

Carman R, Aigars J, Larsen B (1996) Carbon and nutrient geochemistry of the surface sediments of the Gulf of Riga, Baltic Sea. Mar Geol 134:57–76. doi:10.1016/0025-3227(96)00033-3

Celi L, Lamacchia S, Marsan FA, Barberis E (1999) Interaction of inositol hexaphosphate on clays: adsorption and charging phenomena. Soil Sci 164(8):574–585. doi:10.1097/00010694-199908000-00005

Chang SC, Jackson ML (1957) Fractionation of soil phosphorus. Soil Sci 84:133–144. doi:10.1097/00010694-195708000-00005

Coey JMD, Schindler DW, Weber F (1974) Iron compounds in lake sediments. Can J Earth Sci 11:1489–1493

Conley DJ, Stockenberg A, Carman R, Johnstone RW, Rahm L, Wulff F (1997) Sediment-water nutrient fluxes in the Gulf of Finland, Baltic Sea. Estuar Coast Shelf Sci 45:591–598. doi:10.1006/ecss.1997.0246

Delaney ML (1998) Phosphorus accumulation in marine sediments and the oceanic phosphorus cycle. Global

Biogeochem Cycles 12(4):563–572. doi:10.1029/98GB02263

Drever JI (2002) The geochemistry of natural waters: surface and groundwater environments, 3rd edn. Prentice Hall, New Jersey, p 436

Edlund G, Carman R (2001) Distribution and diagenesis of organic and inorganic phosphorus in sediments of the Baltic proper. Chemosphere 45:1053–1061. doi:10.1016/S0045-6535(01)00155-2

Einsele W (1936) Über die Beziehungen des Eisenkreislaufs zum Phosphatkreislauf im eutrophen See. Arch Hydrobiol 29:664–686

Einsele W (1938) Über chemische und kolloidchemische Vorgänge in Eisen-Phosphat-Systemen unter limnochemischen und limnogeologischen Gesichtspunkten. Arch Hydrobiol Planktonkd 33:361–387

Emeis K-C, Struck U, Leipe T, Pollehne F, Kunzendorf H, Christiansen C (2000) Changes in the C, N, P burial rates in some Baltic Sea sediments over the last 150 years–relevance to P regeneration rates and the phosphorus cycle. Mar Geol 167:43–59. doi:10.1016/S0025-3227(00)00015-3

Frankowski L, Bolałek J, Szostek A (2002) Phosphorus in bottom sediments of Pomeranian Bay (Southern Baltic-Poland). Estuar Coast Shelf Sci 54:1027–1038. doi:10.1006/ecss.2001.0874

Froelich PN (1988) Kinetic control of dissolved phosphate in natural rivers and estuaries: aprimer on the phosphate buffer mechanism. Limnol Oceanogr 33(4–2):649–668

Grasshoff K (1983) Determination of oxygen. In: Grasshoff K, Ehrhardt M, Kremling K (eds) Methods of seawater analysis, 2nd edn. Verlag Chemie Gmbh, Weinheim, pp 61–72

Hansen HP, Koroleff F (1999) Determination of nutrients. In: Grasshoff K, Kremling K, Ehrhardt M (eds) Methods of seawater analysis, 3rd edn. Verlag Chemie Gmbh, Weinheim, pp 159–228

Hartikainen H (1979) Phosphorus and its reactions in terrestrial soils and lake sediments. J Sci Agric Soc Finl 51(8):537–624

HELCOM (2003) The Baltic marine environment 1999–2002. Baltic Sea environment proceedings no. 87. Erweko Painotuote Oy, Helsinki, p 47

Hieltjes AHM, Lijklema L (1980) Fractionation of inorganic phosphates in calcareous sediments. J Environ Qual 9(3):405–407

Hietanen S, Laine AO, Lukkari K (2007) The complex effects of the invasive polychaetes *Marenzelleria* spp. on benthic nutrient dynamics. J Exp Mar Biol Ecol 352:89–102. doi:10.1016/j.jembe.2007.07.018

Hingston FJ, Atkinson RJ, Posner AM, Quirk JP (1967) Specific adsorption of anions. Nature 215:1459–1461. doi:10.1038/2151459a0

Hupfer M, Rübe B, Schmieder P (2004) Origin and diagenesis of polyphosphate in lake sediments: a $^{31}$P-NMR study. Limnol Oceanogr 49(1):1–10

Hyacinthe C, Van Cappellen P (2004) An authigenic iron phosphate phase in estuarine sediments: composition, formation and chemical reactivity. Mar Chem 91:227–251. doi:10.1016/j.marchem.2004.04.006

Ingall E, Clark L (1998) Redox-dependent phosphorus cycling: microbial and abiotic processes. Mineral Mag 62A:677–678. doi:10.1180/minmag.1998.62A.2.23

Ingall E, Jahnke R (1994) Evidence for enhanced phosphorus regeneration from marine sediments overlain by oxygen depleted waters. Geochim Cosmochim Acta 58(11):2571–2575. doi:10.1016/0016-7037(94)90033-7

Ingall ED, Bustin RM, Van Cappellen P (1993) Influence of water column anoxia on the burial and preservation of carbon and phosphorus in marine shales. Geochim Cosmochim Acta 57:303–316. doi:10.1016/0016-7037(93)90433-W

Jensen HS, Thamdrup B (1993) Iron-bound phosphorus in marine sediments as measured by bicarbonate-dithionite extraction. Hydrobiologia 253:47–59. doi:10.1007/BF00050721

Jensen HS, Mortensen PB, Andersen FØ, Rasmussen E, Jensen A (1995) Phosphorus cycling in a coastal marine sediment, Aarhus Bay, Denmark. Limnol Oceanogr 40(5):908–917

Jørgensen BB (1977) The sulfur cycle of a coastal marine sediment (Limfjorden, Denmark). Limnol Oceanogr 22(5):814–832

Kamp-Nielsen L (1992) Benthic-pelagic coupling of nutrient metabolism along an estuarine eutrophication gradient. Hydrobiologia 235/236:457–470. doi:10.1007/BF00026234

Kankaanpää H, Vallius H, Sandman O, Niemistö L (1997) Determination of recent sedimentation in the Gulf of Finland using 137-Cs. Oceanol Acta 20(6):823–836

Kemp ALW (1971) Organic carbon and nitrogen in the surface sediments of Lakes Ontario, Erie and Huron. J Sediment Petrol 41(2):537–548

Koistinen T, Stephens MB, Bogatchev V, Nordgulen Ø, Wennerström M, Korhonen J (2001) Geological map of the Fennoscandian shield, scale 1:2,000,000. Geological Surveys of Finland, Norway, and Sweden and the Ministry of Natural Resources of Russia. Espoo, Trondheim, Uppsala, Moscow

Koroleff F (1983) Determination of phosphorus. In: Grasshoff K, Ehrhardt M, Kremling K (eds) Methods of seawater analysis, 2nd edn. Verlag Chemie Gmbh, Weinheim, pp 125–142

Koski-Vähälä J, Hartikainen H, Tallberg P (2001) Phosphorus mobilization from various sediment pools in response to increased pH and silicate concentration. J Environ Qual 30:546–552

Kotilainen A, Vallius H, Ryabchuk D (2007) Seafloor anoxia and modern laminated sediments in coastal basins of the eastern Gulf of Finland, Baltic Sea. In: Vallius H (ed) Holocene sedimentary environment and sediment geochemistry of the eastern Gulf of Finland, Baltic Sea. Geological Survey of Finland, Special Paper 45, Espoo, pp 49–62

Krom MD, Berner RA (1980) Adsorption of phosphate in anoxic marine sediments. Limnol Oceanogr 25(5):797–806

Krom MD, Berner RA (1981) The diagenesis of phosphorus in a nearshore marine sediment. Geochim Cosmochim Acta 45:207–216. doi:10.1016/0016-7037(81)90164-2

Kullenberg G (1981) Physical oceanography. In: Vopio A (ed) The Baltic Sea. Elsevier Oceanography Series, 30, Netherlands, pp 135–181

Kyzyurov V, Mikheev Y, Niemistö L, Winterhalter B, Häsänen E, Ilius E (1994) Shipboard determination of deposition rates of recent sediments based on Chernobyl derived Cesium-137. Baltica 8:64–67

Lee GF, Sonzogni WC, Spear RD (1977) Significance of oxic vs. anoxic conditions for Lake Mendota sediment phosphorus release. In: Golterman HL (ed) Interactions between sediments and fresh water. Dr W Junk BV, The Hague, pp 294–306

Lehtoranta J (1998) Net sedimentation and sediment-water nutrient fluxes in the eastern Gulf of Finland (Baltic Sea). Vie Milieu 48(4):341–352

Leivuori M (2000) Distribution and accumulation of metals in sediments of the northern Baltic Sea. Finnish Institute of Marine Research—contributions, no. 2. Dissertation, University of Helsinki

Lopez P (2004) Spatial distribution of sedimentary phosphorus pools in a Mediterranean coastal lagoon 'Albufera d'es Grau' (Minorca Island, Spain). Mar Geol 203:161–176. doi:10.1016/S0025-3227(03)00333-5

Loring DH, Rantala RTT (1992) Manual for the geochemical analyses of marine sediments and suspended particulate matter. Earth Sci Rev 32:235–283. doi:10.1016/0012-8252(92)90001-A

Louchouarn P, Lucotte M, Duchemin E, de Vernal A (1997) Early diagenetic processes in recent sediments of the Gulf of St-Lawrence: phosphorus, carbon and iron burial rates. Mar Geol 139:181–200. doi:10.1016/S0025-3227(96)00110-7

Lukkari K, Hartikainen H, Leivuori M (2007) Fractionation of sediment phosphorus revisited. I: fractionation steps and their biogeochemical basis. Limnol Oceanogr Methods 5:433–444

Lukkari K, Leivuori M, Hartikainen H (2008) Vertical distribution and chemical character of sediment phosphorus in two shallow estuaries in the Baltic Sea. Biogeochemistry 90(2):171–191. doi:10.1007/s10533-008-9243-2

Lukkari K, Leivuori M, Kotilainen A (submitted) The chemical character and behaviour of phosphorus in poorly oxygenated sediments from open sea to organic-rich inner bay in the Baltic Sea

Mäkelä K, Tuominen L (2003) Pore water nutrient profiles and dynamics in soft bottoms of the northern Baltic Sea. Hydrobiologia 492:43–53. doi:10.1023/A:1024809710854

Martens CS, Goldhaber MB (1978) Early diagenesis in transitional sedimentary environments of the White Oak River Estuary, North Carolina. Limnol Oceanogr 23(3):428–441

Mattila J, Kankaanpää H, Ilus E (2006) Estimation of recent sediment accumulation rates in the Baltic Sea using artificial radionuclides 137Cs and 239, 240Pu as time markers. Boreal Environ Res 11:95–107

Mortimer CH (1941) The exchange of dissolved substances between mud and water in lakes, I. J Ecol 29:280–329. doi:10.2307/2256395

Mortimer CH (1942) The exchange of dissolved substances between mud and water in lakes, II. J Ecol 30:147–201. doi:10.2307/2256691

Mortimer CH (1971) Chemical exchanges between sediments and water in the Great Lakes–speculations on probable regulatory mechanisms. Limnol Oceanogr 16(2):387–404

Paludan C, Jensen HS (1995) Sequential extraction of phosphorus in freshwater wetland and lake sediment: significance of humic acids. Wetlands 15(4):365–373

Peltovuori T (2006) Phosphorus in agricultural soils of Finland—characterization of reserves and retention in mineral soil profiles. Pro Terra No 26. Dissertation, University of Helsinki

Persson J, Jonsson P (2000) Historical development of laminated sediments–an approach to detect soft sediment ecosystem changes in the Baltic Sea. Mar Pollut Bull 40:122–134. doi:10.1016/S0025-326X(99)00180-0

Petr T (1977) Bioturbation and exchange of chemicals in the mud-water interface. In: Golterman HL (ed) Interactions between sediments and fresh water. Proceedings of an international symposium held at Amsterdam, the Netherlands, September 6–10, 1976. Dr W Junk BV, The Hague. pp 216–226

Pettersson K, Boström B, Jacobsen O-S (1988) Phosphorus in sediments—speciation and analysis. Hydrobiologia 170: 91–101

Psenner R, Pucsko R, Sager M (1984) Die Fraktionierung organischer und anorganischer Phosphorverbindungen von Sedimenten. Versuch einer Definition ökologisch wichtiger Fraktionen. Fractionation of organic and inorganic phosphorus compounds in lake sediments. An attempt to characterize ecologically important fractions. Arch Hydrobiol Suppl 70(1):111–155

Redfield AC, Ketchum BH, Richards FA (1963) The influence of organisms on the composition of sea-water. In: Hill MN (ed) The sea: ideas and observations on progress in the study of the seas, vol 2. The composition of sea-water: comparative and descriptive oceanography. Interscience, New York, pp 26–77

Reitzel K, Ahlgren J, Gogoll A, Jensen HS, Rydin E (2006) Characterization of phosphorus in sequential extracts from lake sediments using $^{31}$P nuclear magnetic resonance spectroscopy. Can J Fish Aquat Sci 63:1686–1699. doi:10.1139/F06-070

Reitzel K, Ahlgren J, DeBrabandere H, Waldebäck M, Gogoll A, Tranvik L, Rydin E (2007) Degradation rates of organic phosphorus in lake sediment. Biogeochemistry 82:15–28. doi:10.1007/s10533-006-9049-z

Ruban V, López-Sánchez JF, Pardo P, Rauret G, Muntau H, Quevauviller P (1999) Selection and evaluation of sequential extraction procedures for the determination of phosphorus forms in lake sediment. J Environ Monit 1:51–56. doi:10.1039/a807778i

Ruttenberg KC (1992) Development of a sequential extraction method for different forms of phosphorus in marine sediments. Limnol Oceanogr 37(7):1460–1482

Ruttenberg KC, Goñi MA (1997) Depth trends in phosphorus distribution and C:N:P ratios of organic matter in Amazon Fan sediments: indices of organic matter source and burial history. In: Flood RD, Piper DJW, Klaus A, Peterson LC (eds) Proceedings of the ocean drilling program, 1997, scientific results, vol 155. pp 505–517

Ryden JC, Syers JK, Tillman RW (1987) Inorganic anion sorption and interactions with phosphate sorption by

hydrous ferric oxide gel. J Soil Sci 38:211–217. doi:10.1111/j.1365-2389.1987.tb02138.x

Schnitzer M (1969) Reactions between fulvic acid, a soil humic compound and inorganic soil constituents. Soil Sci Soc Am Proc 33:75–81

Shukla SS, Syers JK, Williams JDH, Armstrong DE, Harris RF (1971) Sorption of inorganic phosphate by lake sediments. Soil Sci Soc Am Proc 35:244–249

Slomp CP, Epping EHG, Helder W, Van Raaphorst W (1996a) A key role for iron-bound phosphorus in authigenic apatite formation in North Atlantic continental platform sediments. J Mar Res 54:1179–1205. doi:10.1357/002224096321374 5

Slomp CP, Van der Gaast SJ, van Raaphorst W (1996b) Phosphorus binding by poorly crystalline iron oxides in North Sea sediments. Mar Chem 52:55–73. doi:10.1016/0304-4203(95)00078-X

Stepanauskas R, Jørgensen NOG, Eigaard OR, Žvikas A, Tranvik LJ, Leonardson L (2002) Summer inputs of riverine nutrients to the Baltic Sea: bioavailability and eutrophication relevance. Ecol Monogr 72(4):579–597

Stumm W, Morgan JJ (1996) Aquatic chemistry. Chemical equilibria and rates in natural waters, 3rd edn. Wiley, New York, p 1022

Suzumura M, Kamatani A (1995) Mineralization of inositol hexaphosphate in aerobic and anaerobic marine sediments: implications for the phosphorus cycle. Geochim Cosmochim Acta 59(5):1021–1026. doi:10.1016/0016-7037(95)00006-2

Vaalgamaa S, Conley DJ (2008) Detecting environmental change in estuaries: nutrient and heavy metal distributions in sediment cores in estuaries from the Gulf of Finland, Baltic Sea. Estuar Coast Shelf Sci 76:45–56. doi:10.1016/j.ecss.2007.06.007

Vallius M (1999) Recent sediments of the Gulf of Finland: an environment affected by the accumulation of heavy metals. Dissertation, Åbo Akademi University, p 43

Vallius H (2006) Permanent seafloor anoxia in coastal basins of the northwestern Gulf of Finland, Baltic Sea. Ambio 35(3):105–108. doi:10.1579/0044-7447(2006)35[105:PSAICB]2.0.CO;2

Van Eck GTM (1982) Forms of phosphorus in particulate matter from the Hollands Diep/Haringvliet, The Netherlands. Hydrobiologia 92:665–681

Virtasalo JJ, Kotilainen AT (2008) Phosphorus forms and reactive iron in lateglacial, postglacial and brackish-water sediments of the Archipelago Sea, northern Baltic Sea. Mar Geol 252:1–12. doi:10.1016/j.margeo.2008.03.008

Virtasalo JJ, Kohonen T, Vuorinen I, Huttula T (2005) Sea bottom anoxia in the Archipelago Sea, northern Baltic Sea—implications for phosphorus remineralization at the sediment surface. Mar Geol 224:103–122. doi:10.1016/j.margeo.2005.07.010

Williams JDH, Mayer T (1972) Effects of sediment diagenesis and regeneration of phosphorus with special reference to Lakes Erie and Ontario. In: Allen HE, Kramer JP (eds) Nutrients in natural waters. Wiley, New York, pp 281–315

Williams JDH, Syers JK, Armstrong DE, Harris RF (1971a) Characterization of inorganic phosphate in noncalcareous lake sediments. Soil Sci Soc Am Proc 35:556–561

Williams JDH, Syers JK, Shukla SS, Harris RF, Armstrong DE (1971b) Levels of inorganic and total phosphorus in Lake Sediments as related to other sediment parameters. Environ Sci Technol 5(11):1113–1120. doi:10.1021/es60058a001

Williams JDH, Jaquet J-M, Thomas RL (1976) Forms of phosphorus in the surficial sediments of Lake Erie. J Fish Res Board Can 33(3):413–429

Winterhalter B, Flodén T, Ignatius H, Axberg S, Niemistö L (1981) Geology of the Baltic Sea. In: Vopio A (ed) The Baltic Sea. Elsevier oceanography series, 30, Netherlands, pp 1–121